

# Advantages and Limitations of Combined Diffusion-Phase Equilibrium Modelling for Pressure–Temperature–Time History of Metamorphic Rocks

Shah Wali Faryad <sup>1,\*</sup>, Josef Ježek<sup>1</sup> and James A. D. Connolly <sup>2</sup>

<sup>1</sup>Faculty of Science, Charles University, Albertov 6, 128 43 Prague 2, Czech Republic

<sup>2</sup>Department of Earth Sciences, ETU Zurich, Sonneggstr 5, CH-8092 Zurich, Switzerland

\*Corresponding author. E-mail: faryad@natur.cuni.cz

## Abstract

This paper presents and discusses the results of phase diagram (Perple\_X) and diffusion modelling (CZGM, or Compositional Zoning and its Modification by diffusion) to constrain the P–T path of metamorphism. The approach is based on the best fits between the zoning profile in measured garnet and that obtained by the intersections of garnet isopleths calculated by phase diagram modelling using whole rock bulk composition. The model was applied to garnets in natural rocks of various metamorphic grades, which were formed within different geotectonic environments. To compare the sequence of compositional change during Barrovian-type metamorphism, well-studied pelitic rocks from garnet–staurolite, kyanite–sillimanite, and sillimanite–K-feldspar metamorphic zones were selected. Garnets with two-stepped core and rim profiles that were formed during two different metamorphic stages or events were used for pressure–temperature (P–T) path constraint of each stage or event. For high-grade rocks, in which the original zoning profile in garnet was severely modified, the diffusion of the initial zoning profile was quantified to estimate the timescale of the metamorphic event. These rocks include high- to ultra-high-pressure rocks, which were subjected to thermal overprinting during collisional orogenesis. The results of the application of this approach allow for deciphering the reason why the calculated profile by phase diagram modelling does not fit with that of the measured garnet from low-grade rocks, in which garnet has preserved the original compositional zoning. This includes garnets whose nucleation was shifted from the garnet-in boundary to higher temperatures and pressures, as well as garnet crystallised during different metamorphic stages or events. Finally, the P–T paths in high-grade rocks were constrained after the multicomponent diffusion in garnet was quantified, and this was used for further P–T-time path constraint of metamorphism in the rocks.

**Keywords:** P–T path constraint, metamorphic rocks, garnet zoning

## INTRODUCTION

Phase equilibrium modelling is a common method for estimating the pressure–temperature (P–T) conditions of metamorphism (de Capitani, 1994; Connolly, 2005; Holland & Powell, 2011). As stability fields of minerals can cover large P–T ranges, the calculated compositional isopleths of garnet are most often used to locate the P–T conditions reached during metamorphism. However, the match between predicted (calculated) and observed compositions (measured profile) in garnet is generally imperfect. The mismatch may be due to many factors, but the most common explanation in high-grade rocks is the modification of the initial zoning profiles in garnet by diffusion (e.g. Loomis *et al.*, 1985; Chakraborty & Ganguly, 1992; Ganguly *et al.*, 1998). Discrepancy between calculated and measured profiles can also occur in garnet from low- to medium-grade rocks, in which no or minimum diffusion is expected. If there is no information about three-dimensional imaging of the garnet grain (e.g. Daniel & Spear, 1998; Gaidies & George, 2021), then it is difficult to explore whether the mismatch is due to the cut effect, in which the analysed profile does not

cross the core of the garnet crystal, or as result of incomplete equilibration.

A number of approaches have been developed to predict the chemical-zoning pattern of garnet growing in equilibrium with a given set of phases along a specific pressure–temperature–time (P–T–t) path. This includes the computer program DiffGibbs (Florence & Spear, 1991; Spear *et al.*, 1991), which accounts for chemical fractionation during garnet growth as well as for intra-granular diffusion in garnet. This procedure was further improved by Gaidies *et al.* (2008), who developed the Theria-G software by combining diffusion modelling with the Theriak-Domino software (de Capitani, 1994) to simulate initial and diffusional compositional profiles during prograde garnet growth. The preservation of garnet of various sizes, temperatures, and times has been modelled by many authors (e.g. Loomis, 1986; Chakraborty & Ganguly, 1991; Perchuk & Gerya, 2005; Caddick *et al.*, 2010). Another software known as CZGM (Compositional Zoning and its Modification during metamorphism) (Faryad & Ježek, 2019) partially adopts the method by Gaidies *et al.* (2008), yet also combines the

phase diagram section by *Perple\_X* (Connolly, 2005) and diffusion modelling (Faryad & Chakraborty, 2005). Importantly, the CZGM allows the creation of a P–T path of metamorphism based on the zoning profiles in garnet both in low-grade rock with no or minimum diffusion, as well as in partially modified zoning profiles in garnet from high-grade rocks.

In pelitic rocks subject to Barrovian-type metamorphism, mineral growth is accompanied by dehydration reactions among the fine-grained matrix phases, thus the observed measured profile of garnet composition from low-grade rocks tends to fit well with that obtained by intersections of the isopleths determined by phase diagram calculation. However, in semipelitic rocks, in which parts of the bulk rock composition are isolated, the presence of relict phases can act as barrier for mineral growth and result in reaction overstepping (path 1 in Fig. 1). In that case, the core composition of the measured garnet ( $c_1$ ) is shifted from the calculated garnet-in boundary ( $c_2$ ) to reflect higher temperature and/or pressure. A similar or more extreme situation in terms of the delay of new mineral formation can also occur if dry and competent igneous or metamorphic basement rocks are subject to metamorphism. The best-known examples are from granulite facies rocks in the Western Gneiss complex (Austrheim, 1987) and from gabbros in the Eastern Alps (Proyer & Postl, 2010), where the recrystallisation of the rocks occurred after they reached eclogite facies conditions. Moreover, further complexity in constraining P–T paths can occur if garnet growth occurred during two or more stages or metamorphic events (path 2, Fig. 1). In addition to the isolation of parts of the bulk chemistry of minerals formed during the first event, the effective bulk chemistry is needed for the formation or regrowth of garnet during the second event. Finally, in high-grade rocks, the constraint of the P–T path can be complicated if the garnet formed by any of the above process was subjected to modification by diffusion (path 3, Fig. 1). In that case, the whole, or at least the core and rim parts, of the measured profile can deviate from that obtained by phase equilibrium calculation.

In this work, we present a series of examples of zoned garnets in natural metamorphic rocks which highlight the complexities between zoning in the measured garnet and garnet isopleths, calculated from the whole bulk rock using phase equilibrium modelling. We aim to draw attention to the limitations of the phase diagram calculation and to find a possible solution for how to deal with the discrepancy between the calculated and measured compositional profiles of garnet in metamorphic rocks. Through application of the CZGM (Compositional Zoning and its Modification by diffusion) software, we examine garnet zoning formed during a single episode of Barrovian-type metamorphism, as well as garnet in polymetamorphic rocks, to constrain the P–T paths of metamorphism by comparing the initial zoning profiles (calculated using phase equilibrium modelling) with the measured profiles in garnet. We clarify why the measured core-to-rim profiles in garnet, which are either not affected or less affected by diffusion, do not fit with the calculated (initial) profiles in low- to medium-grade rocks. We also analyse the preservation and/or modification of major element zoning that is created either during prograde metamorphism or by being subjected to diffusion at different P–T–t (time) relations.

## METHODOLOGY

Pressure–temperature path constraint of a metamorphic event by modelling phase equilibrium and compositional zoning in garnet consists of finding the intersections of isopleths in the P–T diagram that correspond to the compositions along the measured

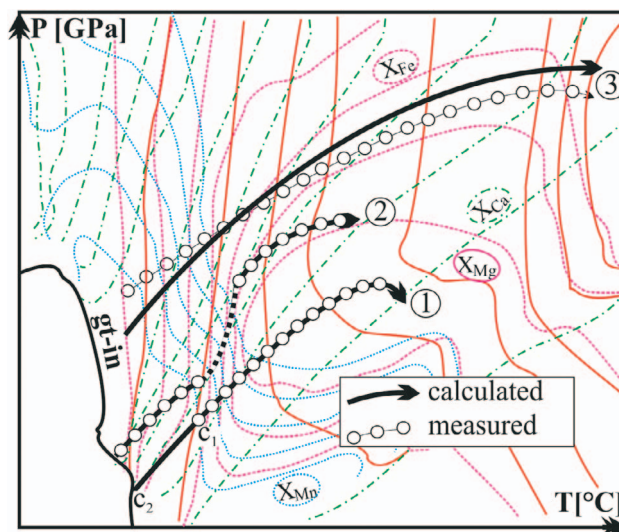


**Fig. 1.** Illustrative examples indicating differences in P–T paths of metamorphic rocks obtained based on the best fits between compositional zoning in measured garnets and intersections of the calculated garnet isopleths ( $X_{Fe}$ ,  $X_{Mn}$ ,  $X_{Mg}$ ,  $X_{Ca}$ ,  $X_{Fe} = Fe^{2+}/(Fe^{2+} + Mn + Mg + Ca)$ ). Path (1) shows a shift in P–T conditions between core composition in the measured garnet ( $c_1$ ) and that calculated using phase diagram modelling ( $c_2$ ). In path (2), the zoning profile in the measured garnet fits in two sections (near the core and rim) with the calculated profile. The section in between (thick dotted) is interpolated. Paths 1 and 2 are from garnet in low-grade rock, where prograde zoning in garnet was not modified. In high-grade rock, where garnet zoning was modified (path 3), compositions of the measured profile in garnet differ from that obtained by the intersections of the calculated isopleths.

profile in the garnet. This is possible for garnet of isometric shape and concentric zoning, which grew in equilibrium with the matrix and whose original zoning profile was not modified by diffusion. However, the finding of the isopleth intersections, which fit along the whole length of the profile, is not an easy task. In most cases, intersections of isopleths with similar compositions are obtained only for cores and rims of the measured profile. In addition, core composition in the measured garnet may not fit with the calculated garnet-in boundary. In high-grade metamorphic rocks, the original zoning profiles is obviously modified, and the solution requires quantification of diffusion prior to finding the best fit between measured and calculated profiles. To overcome this problem, most common examples of garnet formed in different source rocks and subjected to one or more metamorphism events were selected for this study. The approach of CZGM software (Faryad & Ježek, 2019) was applied to simulate the initial compositional profiles of garnet, obtained by *Perple\_X* with the application of garnet fractionation, in combination with multicomponent diffusion along a selected P–T path during prograde metamorphism and subsequent decompression and/or cooling. It should be noted that this approach considers that the measured garnet crystal has an isometric shape with a concentric profile along the section, which crosses the geometric core of the crystal. Other possible kinetic factors (like deformation, fluid, heating rate, nucleation, Loomis, 1979; Dempster et al., 2018), which control garnet growth or resorption/consumption of garnet during its stability field are not considered in this approach and in the CZGM software.

The garnet examples selected for this study met a number of criteria regarding their origin and compositional zoning and the degree of metamorphism of the host rocks. This includes simple zoning garnets formed during a single metamorphic event as

well as garnet with complex zoning and created by multistage or polymetamorphic events. It was also important to know whether recrystallization of the rock occurred at or before the garnet-in boundary or whether the garnet-forming process was shifted to higher temperature and/or pressure conditions. Since the selected examples come from our own studies and from the literature, it was essential to know about field relationships of the rocks and possibly about the age of metamorphism. The examples with simple zoning garnet come from three Barrovian-type metapelites, which underwent different degrees of metamorphism: low-grade rocks with well-preserved prograde zoning garnet, middle-grade rocks with garnet partially affected by diffusion, and high-grade rocks with strongly modified zoning profile of garnet. In addition to the P–T path constraint, the objective for the low-grade rock experiment was to verify whether the measured core of the garnet fit with the garnet-in boundary calculated by the phase diagram calculation; and further, in the case that they did not fit, to explain the reason for the discrepancy. For the high-grade rocks, the compositionally modified zoning profile in garnet was used to estimate the duration of metamorphism within the garnet stability field that was reached by the rocks. In addition, two garnets in polymetamorphic rocks formed during Barrovian-type metamorphism and a subsequent high-pressure collisional event were also analysed to illustrate the effect of bulk rock fractionation during the two garnet-forming events. Three examples of the garnets (two in metabasic rocks and one in felsic rock) were formed during subduction and subsequent collisional events and are indicative of the most typical garnet-forming process in eclogite facies rocks, with possible thermal overprinting. The garnet in the metabasic rocks involved both hydrated source material and dry igneous rock, in which garnet formed in the coesite stability field due to reaction overstepping. The dry mafic and felsic rocks contained partially modified garnet by diffusion with regrowth owing to heating during exhumation.

In the case of examples taken from the literature, we repeat the thermobarometric analysis to see to what extent the original results are modified by our choice of thermodynamic data and computational methods. Specifically, we use the thermodynamic data base of [Holland & Powell \(2011\)](#) with solution models for chlorite, chloritoid, biotite, mica, garnet, staurolite, cordierite, ilmenite, and melt from [White et al. \(2014\)](#) and that of feldspar from [Benisek et al. \(2010\)](#), while the phase equilibria are predicted by free energy minimisation ([Connolly, 2009](#)). The selected samples from the literature are from Barrovian-type metapelite of the garnet–staurolite zone in the Sikkim Himalaya ([Gaidies et al., 2015](#)), sillimanite-zone metapelite of eastern Tibet ([Weller et al., 2013](#)), and granulite facies pelitic rocks of the Damara Belt, Namibia ([Jung et al., 2019](#)).

The measured profiles in garnet from each selected sample were first tested by CZGM based on the preliminary P–T path to see if their original zoning was modified by diffusion, i.e. if the calculated initial profile differs from that measured in garnet. In the case of preservation of the original zoning (from the garnet–staurolite zone), the best fits between the measured and calculated profiles were obtained using the procedure described below and given in [Faryad & Ježek \(2019\)](#). The basis of this procedure is to constrain a P–T path, which passes through the intersection of calculated compositional isopleths with values similar or close to that of major components along the measured zoning profile from the core to the rim of garnet. It was needed to determine whether the best fit between the measured and calculated profiles is along the whole distance of the zoning profile, or whether the core of the measured profile is shifted to a higher temperature and/or

pressure from the calculated garnet-in boundary. In high-grade rocks (sillimanite zone and granulite), the best fit between measured and initial (original) zoning profiles was calculated after diffusion of the initial profile was quantified. Diffusion quantification was performed using changes of temperature and pressure in the P–T diagram at different time durations.

## P–T PATH CONSTRAINT IN LOW-GRADE ROCKS

To test the best fit between the measured and calculated profiles in garnet from low-grade rock, a sample (24–99) from garnet zone metapelite in Sikkim ([Gaidies et al., 2015](#)) was selected. The rock consists of white mica, quartz, biotite and ilmenite, and the mica together with graphite and chlorite define foliation of the rock. The garnet of isometric shape (1.4 mm in diameter) has well-preserved prograde zoning ([Fig. 2a](#)). [Gaidies et al. \(2015\)](#) calculated, using Theriak/Domino software ([de Capitani & Brown, 1987](#); [de Capitani & Petrakakis, 2010](#)), pressure and temperature of 520°C at 0.45 GPa for the core and 570°C at 0.55 GPa for the rim compositions of garnet. Note that in [Fig. 2a](#), a relative radius of garnet is shown to indicate possible best fits between the measured and calculated profiles. The compositional isopleths ([Fig. 2b and c](#)) of the major divalent cation ratios (values) and mode (volume, [Fig. 1d](#)) are calculated using the bulk rock composition of the sample. As there is no or just minimum diffusion in garnet, it is expected to find intersections of isopleths in the P–T diagram, which closely correspond to those in the measured core-to-rim profile in garnet. The intersections of isopleths corresponding to the composition from core (c) to rim (r) in the measured garnet occur in the P–T interval from ~520°C at 0.5 GPa (core of garnet) to 570°C at 6.0 GPa (rim of garnet). The line connecting these intersection points is the P–T path obtained based on the zoning profile in the measured garnet. However, the starting point of this P–T path is shifted by 30°C and 0.1 GPa to a higher temperature and pressure compared to the calculated garnet-in boundary. If we consider that the phase diagram calculation is correct, then part of the measured profile to the garnet-in boundary is missing ([Fig. 2d](#)). The discrepancy or shift of the calculated core composition from that measured ([Fig. 2b–d](#)) may be attributed to (1) the cut effect, (2) reaction overstepping, or (3) imperfect thermodynamic knowledge. In some cases, the distance of shift can be shortened using different (appropriate) solution models of garnet but calculating the phase diagram for series of samples with different composition of garnet is time consuming. Therefore, we will disregard the imperfect thermodynamic knowledge here and consider whether it is possible to evaluate the significance of the former two options.

### The cut effect in a garnet crystal

If it is not clear whether the analysed section passes through the garnet core e.g. no information from three-dimensional imaging analysis or about cutting of garnet crystal along a plane through the geometric centre, ([Gaidies & George, 2021](#)), the shift of the analysed core from the garnet-in boundary to higher temperature and pressure can be due to the cut effect. Any deviation of the section from a plan through the nucleus, whether that is in the geometric core of the crystal of garnet or not, will result in a miss of the earliest stretch of the measured composition profile, which reveal itself in the calculated composition profiles. [Figure 3](#) shows a schematic illustration of the cut effect in a spherical crystal of garnet with core  $c_1$  and radius  $r_1 = 0.65$  mm that crosses two zones (central zone 1 with radius  $r_3 = 0.24$  mm and outer zone with a

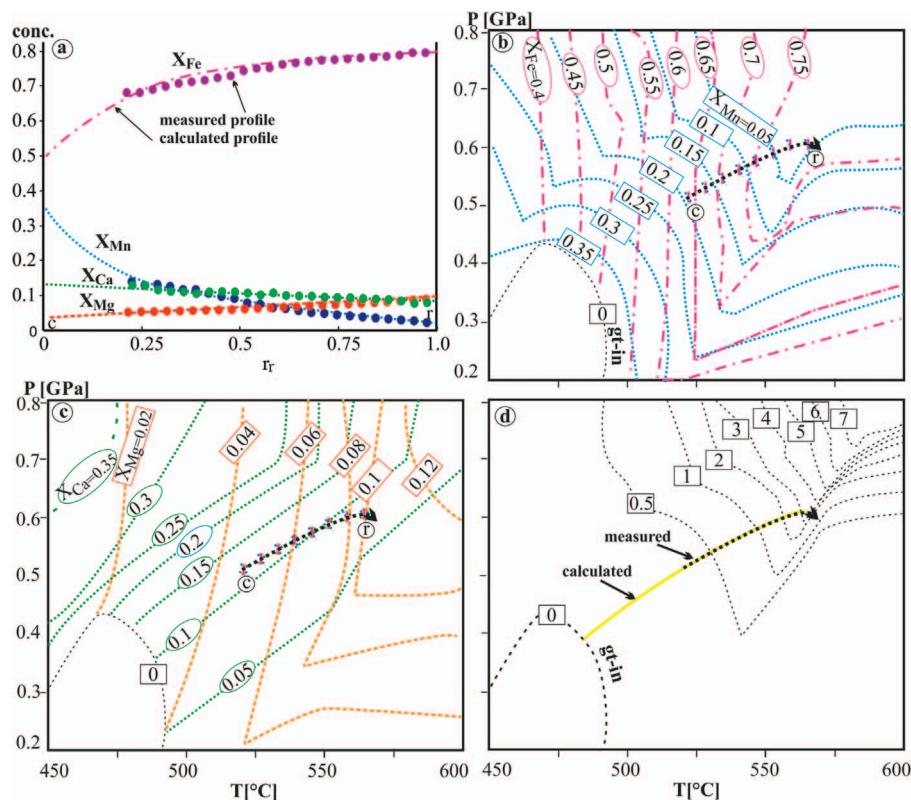


**Fig. 2.** Concentration profiles (core, c to rim, r) in measured garnet (a) and calculated from compositional (b, c) and volume isopleths (d) plotted along relative radius ( $r_r$ ). Compositional zoning in this garnet is not modified and the isopleths for core (c) to rim (r) compositions in the measured garnet intersect each other in the P–T range of  $\sim 520^\circ\text{C}$  at 0.5 GPa to  $570^\circ\text{C}$  at 0.6 GPa (b–d). Part of the calculated (initial) profile (solid curve of yellow colour in d) fits with the measured profile, while the rest of the profile to the garnet-in (gt-in) boundary is extrapolated.

thickness of 0.41 mm, Fig. 3a). Assuming that the garnet crystal nucleated at the garnet-in boundary, the composition in the  $c_1$  core will correspond to that calculated using phase equilibrium modelling. In Fig. 3a, the cut crosses the garnet crystal at the interface between zones 1 and 2 with a distance of  $d = 0.24$  mm (240 microns), relatively far from the real core of the garnet  $c_1$ . The cut does not include zone 1 with radius of  $r_3 = d = 0.24$  mm. The cutting circle with core  $c_2$  and radius  $r_2 = 0.61$  mm covers only zone 2 and is identical to the core-to-rim profile measured in the garnet. The  $r_2$  radius is greater than the actual thickness of the mantle due to its angular deviation from the true radius  $r_1$  and is  $\sim 0.04$  mm shorter than  $r_1$ . The difference in compositional zoning in garnet along both radii  $r_1$  and  $r_2$  in Fig. 3a is indicated along the (normalized) relative radius ( $r_r$ ) in Fig. 3b. The calculated compositional profile (Fig. 3b) was obtained for the selected relative grain size no. 74 in Fig. 3c, which started to grow later than the largest grain no. 100 (for details see Faryad & Ježek, 2019). While the measured profile  $r_2$  covers only zone 2, its composition fits with outer part of  $r_1$  crossing this zone. To compare the composition of the whole measured profile with the calculated one, the length of the measured profile must be compressed so that it fits to the outer part of radius  $r_1$ . This is indicated in Fig. 3d, where the core  $c_2$  of the cut with radius  $r_2$  is shifted along  $r_1$  so that both have the same composition.

The relationships of  $r_1$  (initial or calculated profile) and  $r_2$  (measured profile) in the P–T diagram are similar to that illustrated in Fig. 2b–d. The measured profile coincides with the outer part of the calculated profile, while the central part of the calculated profile to the garnet-in boundary is only interpolation. The  $r_1$  and  $r_2$  relationships could be used to estimate the missing volume

of garnet, which we can consider to be excluded due to the cut effect. If we assume that the radius  $r_1$  in a single crystal corresponds proportionally to the total volume ( $v_1 = \pi \cdot \frac{3}{4} \cdot r_1^3$ ) of garnet formed in the rock, the missing volume (zone 1) resulting from the cut effect will be ( $v_3 = \pi \cdot \frac{3}{4} \cdot r_3^3$ ). We are aware that garnet grains have different sizes and could have nucleated at different times; however, this is only an approximation to understand the volume content not included by the measured profile in Fig. 2b. For garnet with  $r_1 = 0.65$  mm, with the total volume of the garnet being 3.5% among other minerals in the rock, the missing volume with  $r_3 = 0.24$  mm will be only 0.18% of the total volume of the garnet. If distance of the cut from the garnet core is small, with  $d = r_3 = 0.1$  or 0.05 mm, the missing volume  $v_3$  of the total 3.5% volume in the rock will be 0.07% and 0.01%, respectively. This suggests that already a small deviation of the cut from the actual core/nucleus will result in a significant loss of information about the real length of the P–T path and the true composition of nucleus of the garnet.

### Overstepping in garnet nucleation and gradual nucleation

If the cut actually passes through core, and the garnet formed in normal pelitic rocks or rocks in the presence of a free fluid phase, which would enhance the reaction progress (e.g. Putnis *et al.*, 2021), any difference or shift of the core of measured profiles from the calculated garnet-in boundary (similar to that in Fig. 3b–d) can be explained by the actual kinetics of the process, which has two parts that can each be treated as a computationally simple ‘endmember’ scenario: (1) reaction overstepping and (2) gradual nucleation of garnet grains with increasing pressure and temperature. In reaction overstepping, the garnet nucleation

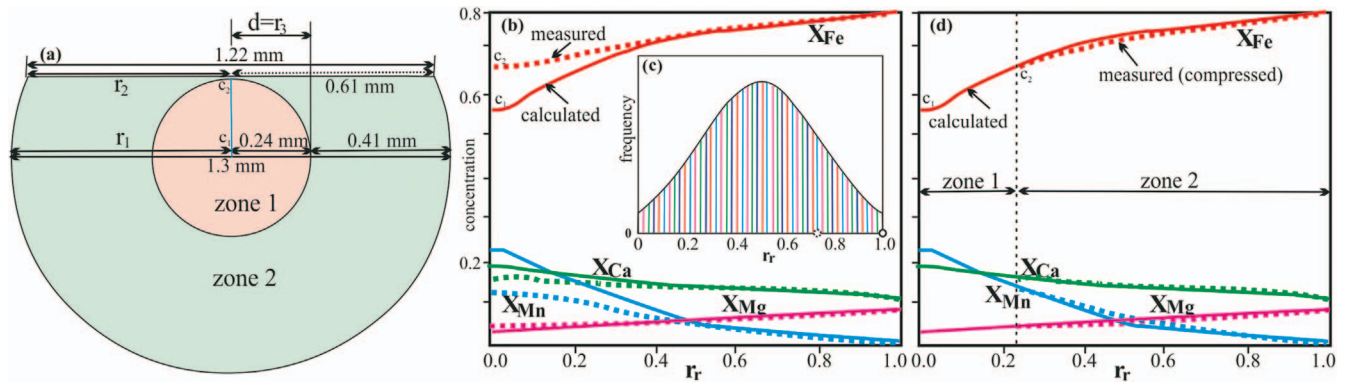


**Fig. 3.** Illustration of cut effect and grain size-nucleation in relations to compositional zoning in garnet. (a) Spherical garnet with a radius of 0.65 mm is cut 24 mm from the garnet core. Note that radius ( $r_2$ ) of the cut circle, along which measured profile was obtained, has a length of 0.61 mm. (b) Core to rim compositions of measured profiles (along the cut radius) and calculated (initial) profiles (along the real radius) are plotted along the relative (normalised) radius. (c) Calculated crystal size distribution, for which large crystals are assumed to nucleate at or near to the boundary of the gt-in field (Fig. 2b) and have a composition corresponding to the garnet core. (d) Best fits of the measured profile with part of the calculated profile from zone 2.

at higher pressure and temperature is due to reaction kinetics, in which garnet-forming reactions are controlled by the excess energy required to make a stable garnet nucleus in heterogeneous environment (e.g. Loomis, 1977; Waters & Lovegrove, 2002; Zeh & Holness, 2003; Castro & Spear, 2017; Spear & Wolfe, 2019). Gradual nucleation means that not all garnet grains in the rock nucleated at the (theoretical or overstepped) garnet-in boundary. In the simplest possible case, when we assume that all these nuclei grow steadily, the resulting grain-size distribution curve would be as shown in Fig. 3c. Large crystals with relative radius of 1.0 nucleated at the beginning of garnet stability field (garnet-in, Fig. 2b), and the grain size was decreasing as the garnet-forming reaction proceeded to higher temperature and pressure conditions. In this case, garnet with a relative radius  $r_r = 1.0$  has a composition corresponding to that calculated from compositional isopleths, while the measured garnet with a relative radius  $r_r \sim 0.76$  (Fig. 3c) nucleated later and does not cover the composition of the most central part of the larger crystal. While a simple reaction overstepping model assumes a certain shift in crystallisation of all garnet grains from the garnet-in boundary to higher P-T conditions, in the model of gradual nucleation, part of the garnet grains have compositions at or near the calculated garnet-in boundary. The best fit solution for measured and calculated compositional profiles for both garnet-forming mechanisms is similar to that with the cut effect in Fig. 3. However, a difference may occur in the case of high P-T overstepping (e.g. garnet nucleation in the coesite field at 600°C, Faryad et al., 2019), while fractionation of the bulk rock does not include garnet crystallisation at the calculated garnet-in boundary.

## MODIFICATION OF THE INITIAL PROFILES

In high-grade rocks, where initial (calculated) compositional zoning in garnet is modified, the best fit solution between the measured and initial profiles is modelled after quantification of the diffusion of the initial profile. Multicomponent diffusion in garnet is modelled using the Fick's-Onsager approach (Onsager, 1945) as a coupled system of diffusion equations. In a spherical coordinate system fixed in the centre of garnet, the equations have the form

$$\frac{\partial C_i}{\partial t} = \frac{1}{r^2} \frac{\partial}{\partial r} \sum_{j=1}^3 D_{ij} r^2 \frac{\partial C_i}{\partial r},$$

where indices  $i=1, 2$ , and 3 correspond to the concentrations of Fe, Mg, and Mn (independent components), while the concentration of Ca (dependent component) is given as  $C_4 = 1 - C_1 - C_2 - C_3$ . Equations are solved numerically by means of a finite difference method. Diffusion coefficients  $D_{ij}$  depend on tracer diffusion coefficients  $D_i^t$ , according to (Lasaga, 1979):

$$D_{ij} = D_i^t \delta_{ij} - \frac{D_i^t C_i}{\sum_{k=1}^4 D_k^t C_k} (D_i^t - D_4^t),$$

where  $\delta_{ij}$  is Kronecker's delta.

The P-T path constraint of garnet with the modified zoning profiles is solved with respect to the boundary conditions. Details about the simulation are described by Faryad & Chakraborty (2005) and Faryad & Ježek (2019). The boundary conditions are solved using the four approaches of (see also <https://www.natur.cuni.cz/geology/petrology/faryad/software-1/software>): (1) open boundary conditions, where garnet rims are assumed to communicate with matrix also after garnet growing stops; (2) closed system, where the zoning profiles are modified depending of the compositional gradient and temperature reached without influx from the outside; (3) fixed boundary conditions, in which the rim compositions remain unchanged after garnet crystallisation stops; and (4) defined boundary conditions by rim compositions in the measured profile. The core-to-rim profile of zoning garnet tends to flatten depending on the compositional gradient along the profile. Figure 4a shows an illustrative example of modification of a compositional profile in garnet by closed boundary conditions, where the initial prograde zoning (solid curves) was modified (dashed curves) due to the compositional gradient between the core and rim. Figure 4b is an example of compositional profile totally homogenised during high-grade metamorphism, after which the rim compositions are modified during cooling. The boundary conditions can either be defined by the user based on the measured profile, or it can follow compositions of the isopleths crossed along the cooling path (Faryad & Ježek, 2019).

## RESULTS

The approach outlined above was applied to (1) garnet formed in a metapelite during a single Barrovian-type metamorphic event

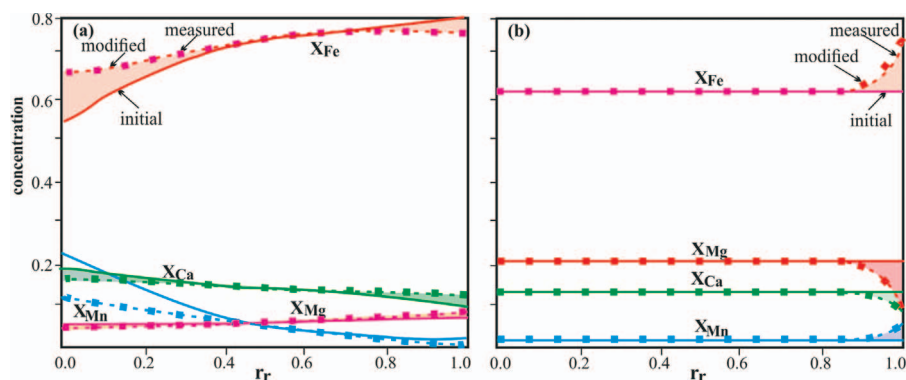


**Fig. 4.** (a) Interpretative example of the best fit solution between measured compositional profiles (large points) and initial profiles (solid curves) after modification by diffusion (dashed curves). The coloured fields indicate the amounts of diffusion of each element that occurred at the core and rim of garnet. (b) Best fit solution of totally homogenised garnet in high-grade rock with the rim subjected to modification during cooling.

in different zones, (2) two garnets with core and rim formed in metapelites during two stages (or two separate metamorphic events), (3) strongly modified garnet in high-grade rocks, and (4) garnet crystallised in dry rocks after a delay in pressure and temperature conditions in respect to the garnet-in boundary. While garnet formation in the first three cases follows the bulk rock or effective bulk rock fractionation, in the last case, the garnet composition and zoning are controlled by material released from the decomposition of the original phases in the rock and by formation of new minerals that become stable at temperatures and pressures reached during recrystallisation of the rock.

## P-T PATH CONSTRAINTS IN BARROVIAN-TYPE METAPELITIC ROCKS

To constrain a P-T paths and assess modification of zoning profiles in garnet during Barrovian-type metamorphism, three zones (garnet–staurolite, kyanite–sillimanite, and sillimanite–K-feldspar) from well-studied areas in the literature were selected. Crucial to this selection was the availability of zoning profiles in a well-developed garnet and bulk rock composition of the host rock used for pseudosection modelling.

### Garnet(–staurolite) zone

For constraining of P-T path of metamorphism in low-grade rocks with well-preserved prograde zoning in garnet, metapelites of the garnet to staurolite zone from the Sikkim Himalaya were selected. The rocks belong to a Barrovian sequence (e.g. Dasgupta *et al.*, 2004; Chakraborty *et al.*, 2016) that experienced a single middle Miocene metamorphism, which, based on Lu-Hf age dating on garnet, occurred in the time span of ~5 Ma (Anczkiewicz *et al.*, 2014). Two samples come from garnet zone (24–99) and garnet–staurolite (SIM5E-12) zone. The first sample (24–99) from garnet zone with well-preserved prograde zoning in garnet was described in the previous section. Based on detailed petrography (Gaidies *et al.*, 2015), the garnet–staurolite zone metapelite (sample SIM5E-12) contains compositionally zoned garnet (up to 5 mm in diameter) that occurs in a well-foliated matrix consisting of white mica, biotite, quartz, plagioclase, and ilmenite. Volumetrically minor staurolite is present in some mica rich layers from the same outcrop. For this rock, P-T conditions of ~530°C at 0.48 GPa to ~575°C at 0.57 GPa were estimated by Gaidies *et al.* (2015) using the Gibbs free energy minimisation approach of the Theriak/Domino software (de Capitani & Brown, 1987; de Capitani & Petrakakis, 2010) and

solution models as follows: garnet and staurolite (Holland & Powell, 1998), feldspar (Baldwin *et al.*, 2005), biotite (White *et al.*, 2005), chloritoid (White *et al.*, 2000), and white mica (Coggon & Holland, 2002). Prograde zoning in garnet was either not at all or only insignificantly modified during this metamorphism (Gaidies *et al.*, 2015).

Phase equilibrium calculations were repeated here for the bulk rock chemistry of sample SIM5E-12, which contains a 4.5 mm diameter garnet that preserves prograde zoning. Based on the computed phase diagram section, the garnet begins to crystallise above 485°C with the composition of  $X_{Mn}=0.35$ ,  $X_{Fe}=0.4$ ,  $X_{Mg}=0.05$ , and  $X_{Ca}=0.1$  (Fig. 5a and b). However, the core-to-rim composition of measured profiles in the garnet match with the intersections of the isopleths in the range of 525°C at 0.52 GPa to 575°C at 0.62 GPa (dotted line in Fig. 5a–c). This indicates a shift of temperature and pressure of ~40°C and 0.15 GPa, reaching higher values for the core composition in the measured garnet compared to that predicted by the phase equilibrium calculations using Perple\_X. It should be noted that this shift is almost twice as high compared to that obtained for this sample by Gaidies *et al.* (2015) using Theriak/Domino and different solution models. Based on the compositional isopleths, ~0.5 vol. % of the total 4 vol. % of garnet should have already formed before reaching 535°C at 0.52 GPa (Fig. 5c). If this P-T path is extrapolated to the garnet-in boundary (485°C at 0.4 GPa), a significant difference occurs in the core compositions between the measured and calculated compositional profiles (Fig. 5d). This would mean that either (1) the garnet zoning was strongly modified by diffusion, (2) the garnet cut is not through the core, or (3) the measured garnet crystallised by reaction overstepping of about 40°C (535–485°C).

To estimate the effect of diffusion in garnet from this zone, we made a series of experiments on this and other samples from this zone. Figure 5e shows positions of the calculated initial (solid lines) and measured profiles (dotted lines) in garnet from sample SIM5E-12. To obtain the best fits along the T-t path (Fig. 5f), very small modification of the  $X_{Mn}$  and  $X_{Fe}$  values near the core and rim parts of the initial profiles were needed. Figure 5g indicates a detail of measured profiles from a strongly zoned garnet in the garnet zone (sample SIM2A-12) that contains white mica, biotite, plagioclase, and ilmenite (Gaidies *et al.*, 2015). The concentration profiles (magnified along the vertical axis) show numerous small-scale compositional oscillations of all major components along the profile. The results of diffusion calculations along the T-time path in Fig. 5f indicate modification of only these small-scale

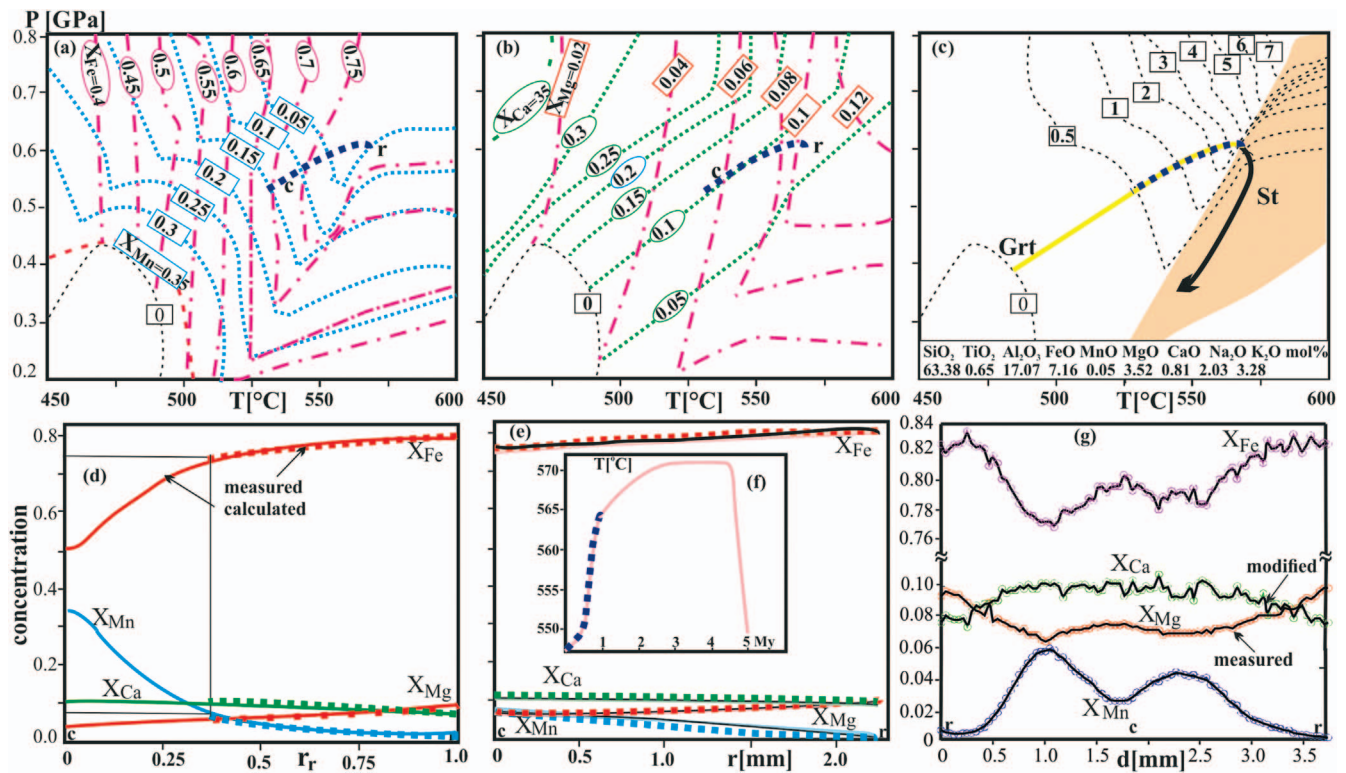


**Fig. 5.** Pressure–temperature path of garnet in garnet–staurolite-zone metapelite (a–e: sample SIM5E-12) from Sikkim. (a–b) Compositional isopleths of garnet and intersections of core to rim values from measured profiles (d). (c) Volume isopleths and P–T path constraint based on the calculated (initial) profiles. The core of calculated profiles (at the gt-in boundary) indicates lower temperature (~485°C at 0.4 GPa) then the core of the measured profile (525°C at 0.52 GPa). This shift suggests that almost 0.5 vol. % of the 4% garnet total in the sample was crystallised prior to the core composition of the measured profiles was formed. (d) Comparison of the calculated and measured profiles are indicated along a relative (normalised) radius. The thin solid lines connect the core compositions in the measured garnet with similar values along the calculated profiles. (e) Best fits between measured profiles (c = core to r = rim) and part of the calculated profiles with similar compositions. Note that the radius is normalised to 2.25 mm. Weak diffusion of  $X_{Mn}$  and  $X_{Fe}$  near cores and rims of the initial profile was calculated based on the T–t path in (f). (g) Measured profile (dots) of garnet (sample SIM2A-12, Gaidies *et al.*, 2015) and its modification (solid) based on the T–t path (f).

oscillations, but the profiles in their entirety remain almost unchanged.

The preservation of original zoning (with minimum diffusion) opens the possibility of looking for other reasons why the core composition of the measured profile does not lie on the calculated garnet-in boundary. As the compositional profile across garnet in sample SIM2E-12 stems from a random section (Gaidies *et al.*, 2015), the shift of P–T conditions between the calculated and measured core of the garnet to the cut effect cannot be excluded. The cut effect can be assessed on whether other measured garnet grains from the same sample are available and whether their core composition is closer to the garnet-in boundary than that selected for calculation. The size distribution of grains in the thin section can also help to determine if the cut of ~0.75 mm distance from the core of the garnet with a radius of 2.25 mm is realistic. In case of the cut effect, the missed radius is calculated both from the missed volume content (~0.5%, Fig. 5c) and by the missed core composition along the measured profiles (Fig. 5d) as predicted by the phase equilibrium calculations. The missed radius (the distance between cut and core of garnet) is estimated from the volume difference as it is explained in Fig. 3a. The result of calculations for the missed volume of 0.5% from the total of 4% (Fig. 5c) indicates  $\Delta r = 0.66$  mm of the total 2.25 mm radius in the measured garnet. In this case, the measured profile (radius) fits only to the outer two third of the calculated radius, normalised to 1.0 (Fig. 5d). The core composition of the measured profile occurs ~one third away from the core of the calculated radius

normalised to 1.0 (thin lines, Fig. 5d). Figure 5e shows the best fit between the measured and the outer half of the calculated radius, both normalised to 2.25 mm. If the cut effect is excluded, the gradual nucleation mechanism can be assessed by analysing several garnet grains to see if some cores show a composition close to that of the calculated garnet-in boundary. The difference between the calculated and measured radius and corresponding volume resulting from gradual nucleation can be solved by a similar method as that used for the cut effect. If the gradual nucleation of the garnet grains is not confirmed, the discrepancy between the measured centre and the calculated garnet-in boundary can be ascribed as the result of reaction overstepping. The procedure for determining the best fit is similar to that of the cut effect.

### Kyanite–sillimanite zone

The selected area with metapelite of kyanite zone comes from the Danba Structural Culmination from eastern Tibet, for which pressure and temperature ranging from 0.45 GPa at 560°C to 0.68 GPa at 680°C have been obtained (Weller *et al.*, 2013). The sample (W126) chosen for this study consists of quartz, plagioclase, biotite, garnet (to 2.5 mm in size), sillimanite, resorbed kyanite, and relicts of staurolite. Garnet shows prograde zoning (Fig. 6a) with a decrease of Mn and a slight increase of Mg in the central part followed by its decrease to the rim. Weller *et al.* (2013) used phase equilibrium modelling in Thermocalc (Holland & Powell, 1998) and calculated pressure and temperature ranging from 0.62–0.68 GPa and 630–660°C for this sample. The solution

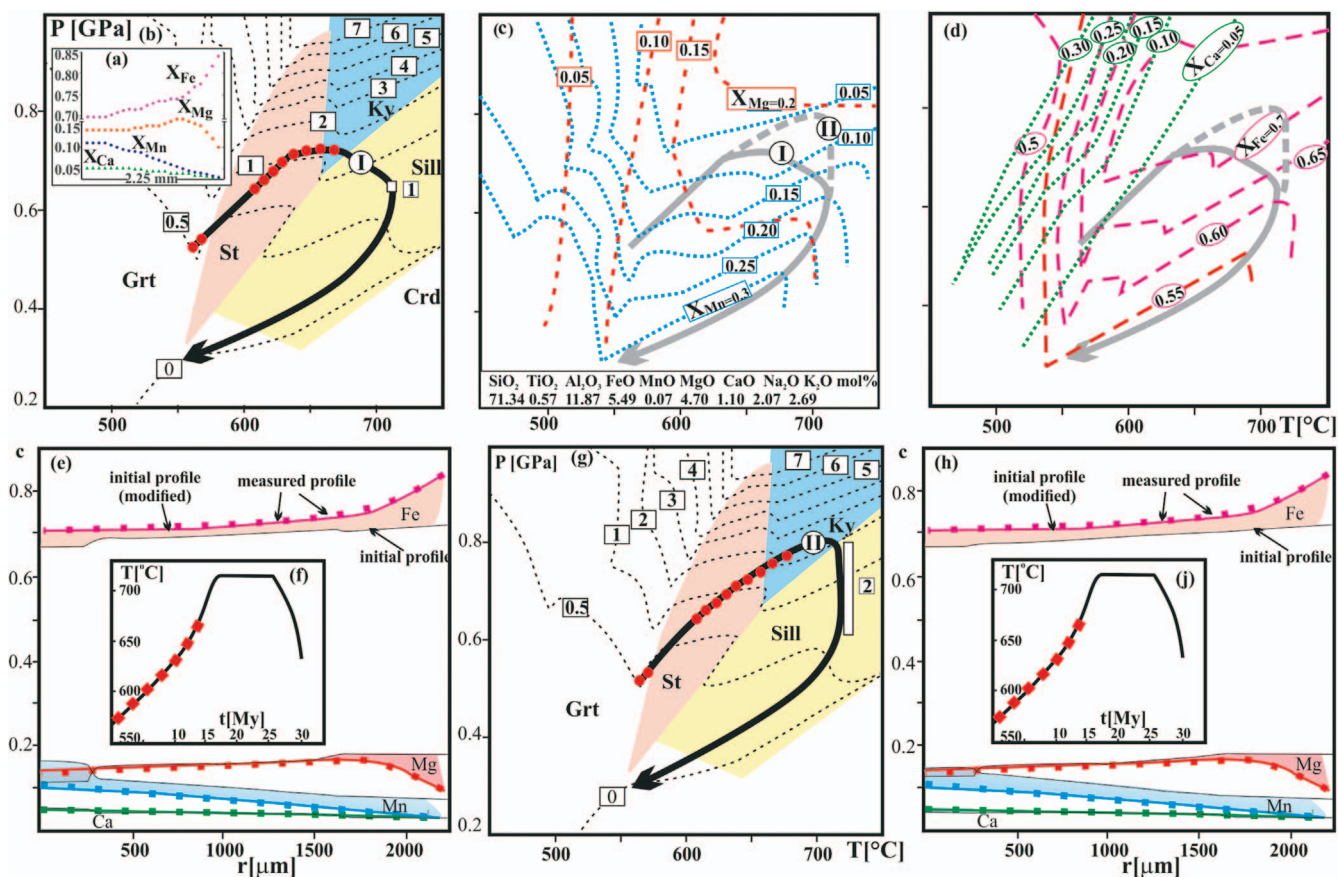


**Fig. 6.** Pressure–temperature path constraint in the kyanite–sillimanite zone with partially modified growth zoning in garnet from Tibet. (a) Measured profile in garnet (multiple elevated). (b) Stability fields of the index phase (staurolite, kyanite, and sillimanite) and calculated volume isopleths of garnet. The solid circles along the P–T path show the position of garnet growth. (c, d) Compositional isopleths with P–T paths (I) calculated based on the best fits (e) between the modified initial profiles and measured profiles and using the T–t path in (f). (g) P–T path (II) constrained based on the best fits (h) between the modified initial profiles and measured profiles and using the T–t path in (j). Note that the 8 Ma relaxation time at 710°C is at constant pressure of 0.64 GPa for path I in Fig. 6b, while for path II in Fig. 6g this thermal relaxation occurs at 710°C during decompression from ~0.8 to 0.6 GPa. Vertical axis in (e, h): c-concentration; horizontal axis: r-normalised radius. Note that the T–t paths (f, j) are similar for both alternative P–T paths I and II.

models used in these calculations were chlorite, chloritoid, and staurolite (Mahar *et al.*, 1997; Holland & Powell, 1998), garnet and biotite (White *et al.*, 2007), and K-feldspar and plagioclase (Holland & Powell, 2003). Based on geochronological dating from monazite, they assumed a duration of metamorphism of about 11 My from the staurolite ( $191.5 \pm 2.4$  Ma) and through the kyanite ( $184.2 \pm 1.5$  Ma) to sillimanite grades ( $179.4 \pm 1.6$  Ma).

The results of the present phase equilibrium modelling in combination with the CZGM program are indicated in Fig. 6. The phase diagram section and compositional isopleths for garnet were calculated in the P–T range of 0.2–1.0 GPa and 450–750°C. Only small amounts of garnet form below 0.8 GPa (Fig. 6b), which show a decrease of Ca and Mn and increase of Mg and Fe with increase of pressure and temperature (Fig. 6c and d). The calculated initial profiles and related P–T path during prograde stage are constrained based on the intersection of the isopleths with concentration values close to those in the measured profiles (Fig. 6a). The rim compositions of the initial profiles in garnet before their modification give a minimum pressure and temperature of 0.72 GPa and 680°C. The corresponding prograde P–T path ranges from 560°C at 0.52 GPa to 680°C at 0.72 GPa, where about 1.5 vol. % of garnet forms in the rock (Fig. 6b).

As modification of compositional profiles by diffusion in garnet is a function of temperature and time, the diffusion equation

is solved by using the calculated maximum temperature and changing of the approximate time duration of metamorphism. For this calculation, we adapted the time span of ~11 Ma (Weller *et al.*, 2013) from the staurolite to the sillimanite grade. Because the rim compositions along the measured profile in garnet show a retrograde (cooling) zoning with a decrease of Mg and increase of Fe and slightly of Mn (Fig. 6a and e), we used boundary conditions as defined by the rim compositions in the measured garnet (see Faryad & Ježek, 2019). This approach modifies the entire profile based on its compositional gradient, but its rim compositions are modified by concentration values defined by the user. Because no cooling time information is available for this rock, a series of cooling times was used to quantify the diffusion that occurred in the garnet so that the calculated modified profile at the rim matched the measured one. Considering similar times for both burial (heating) and exhumation (cooling) of the rocks, a time of 11 My was used for the retrograde stage of cooling from 680°C at 0.72 GPa to 560°C at 0.35 GPa. The results showed that this cooling rate would be not sufficient to reach the best fits with the measured profiles. To achieve the best fits, an additional time of 55 My time for thermal relaxation or isothermal decompression from peak temperature was required. Thermal relaxation is considered to be the time during which the garnet is subject to constant temperature after the end of its growth.

To shorten the relaxation time and to achieve the diffusion required for the best fit, it was needed to increase the peak temperature from 680 to 710°C (Fig. 6a and f). As there is no cordierite in the sample and kyanite occurs only as relict phase, we examined the diffusion calculation along two P–T paths (I, II, Fig. 6c) for a temperature increase of 30°C (680 to 710°C) from the staurolite to the sillimanite grade. In both cases, the cooling and decompression occur in the sillimanite field (Fig. 6b and d). The P–T path (I) follows the temperature increase with a weak decompression, where no additional garnet forms. The relaxation time of ~8 My at peak temperature occurs at almost constant pressure of 0.64 GPa (pint 1 in Fig. 6b). The P–T path (II) assumes heating by continuation of the prograde P–T path with increase of pressure and temperature to 0.8 GPa at 710°C (Fig. 6c and g). In this case, only a small amount (more) garnet forms (total of 2.2 vol. %) at the beginning of extended P–T path (between 660–675°C, Fig. 6g) and further, it becomes parallel to the volume isopleths and no additional garnet forms. The new garnet formed at the rim shows a slight increase of Mg, decrease of Mn and Ca, while Fe remains almost constant (Fig. 6c and d). Considering that the total volume of 2.2 vol. % is proportional to the garnet size with  $r = 2.25$  mm, the new increment of 0.75 vol. % will correspond to a thin (0.25 mm) shell, which will be modified first due to the defined boundary conditions. The advantage of P–T path (II) is that modification of the initial profiles for the period of 8 My at peak temperature occurs along isothermal decompression part (section 2, in Fig. 6g, from 0.8 to 0.55 GPa) of the P–T path. The results of the calculations show no difference in the modification of the garnet profile obtained for P–T paths (I) or (II) (Fig. 6e and h).

### Granulite facies conditions

To analyse modification of compositional zoning in garnet from high-grade rocks, low-pressure cordierite granulite from the Damara Belt, Namibia (Jung *et al.*, 2019), was selected. The metapelite (sample 14NAM01) contains garnet, cordierite, sillimanite, biotite, plagioclase, K-feldspar, and rare ilmenite. Garnet shows only weak retrograde zoning with a decrease of Mg and increase of Fe and Mn towards the rims (Fig. 7a). Calcium is almost flat with a slight increase towards the rims. Jung *et al.* (2019) used Theriak-Domino software of de Capitani & Brown (1987) to estimate a peak pressure and temperature of about 800°C at 0.5 GPa. A clockwise P–T path with partial decompression followed by near-isobaric cooling to <650°C at low pressures of ~3 kbar is inferred based on the cordierite coronas around garnet and rare occurrence of andalusite. Based on geochronological data (Lu–Hf garnet–whole rock and Sm–Nd garnet–whole rock), the authors obtained a range of ages between 500–530 My, based on the assumption that this high-grade metamorphism event lasted around 20–30 My.

We recalculated the initial profiles using *Perple\_X* and simulated their modification by diffusion so as to fit them to the measured profiles in garnet. Our results show the formation of small amounts of garnet in three stages along the constrained P–T path. The first two stages occurred just before and after the staurolite field, and the third stage occurred during the peak P–T conditions in the sillimanite field (Fig. 7b). The initial zoning in garnet from each stage shows a stepwise change of major components, with a decrease of Mn and Ca and increase of Fe and Mg (Fig. 7c–e). Garnet growth ceases along the P–T path at pressure and temperature of 0.46 GPa and 760°C, which are very close to that estimated by Jung *et al.* (2019). The diffusion equation was solved similarly to that in the previous example in Fig. 6, by the adjustment of temperature and/or time to get the

best fits between modified initial profiles and measured profiles. Considering that the peak temperature of 800°C (Jung *et al.*, 2019) was well constrained, this temperature increase should occur by weak decompression or isobaric heating, where no more garnet forms in the rock. However, the use of such high temperature in diffusion modelling would give a duration of metamorphism of about 5 My, which is 4–5 times shorter than the 20–30 My assumed by the previous authors. In addition, such high temperatures would be expected to stabilise a Fe-rich garnet (>0.85, Fig. 7d). Further homogenisation of the initial profiles due to diffusion in an open system (with matrix) would lead to deviation of the calculated Fe profile from that measured profile with Fe ratio of ~0.825.

If we consider that garnet growth stopped by reaching the rim composition of the initial profile at ~750°C and 0.46 GPa and no further heating occurred, the best fit calculations between measured profiles and modified initial profiles would require a longer time compared to that assumed by geochronological data. However, the rim composition of the initial profile reaches the Fe isopleth with a ratio of 0.85, and this can be modified to lower Fe values due to slow cooling. Assuming that the duration of metamorphism of 25–30 My (Jung *et al.*, 2019) is correct, the best fits between simulated initial profiles and measured profiles can be obtained for a P–T loop from 550 at 0.34 GPa to 750°C at 0.45 GPa and back to 525°C at 0.24 GPa (Fig. 7b) along the T–t path of ~27 My with relaxation time of ~3 Ma at peak temperature (Fig. 7f). In addition to cordierite coronas formation, this isothermal decompression at peak temperature could result in partial melting and migmatization in the rocks.

### P–T(–PATH) CONSTRAINT IN ROCKS WITH POLYMETAMORPHIC/MULTISTAGE GARNET GROWTH

In addition to multistage growth of garnet due to mineral reactions during single metamorphic events, the garnet core or central part of the garnet can relate to an older metamorphic event. In both cases, a new garnet with a different composition from the previous one forms due to contrasting P–T conditions. In the case of two metamorphic events, the P–T path for the first event is constrained using bulk rock composition, similar to the process in the previous examples, but any possible resorption and/or modification of the rim composition of the first garnet should be taken into consideration (Faryad *et al.*, 2022). However, when using phase equilibrium modelling and garnet zoning to constrain the P–T path of the second event, several factors must be considered. These include the isolation of relict phase from the reacting bulk rock composition and partial resorption of the first garnet that resulted in releasing of elements to the matrix. In the following, two examples of garnet with different origins and mechanisms of resorption are explained.

### Garnet formed during two metamorphic events

Garnet porphyroblasts (up to 2 cm in size) with two compositionally different central and rim zoning from micaschist in the Austroalpine units (Eastern Alps) are among the best examples defining two metamorphic events (Schuster & Thöni, 1996; Faryad & Chakraborty, 2005; Gaidies *et al.*, 2006). The Austroalpine units represent a south-dipping nappe pile of continental basement and cover rocks, which developed their essential internal nappe structure and main metamorphic overprint during Cretaceous orogenic events (e.g. Frank, 1987; Ratschbacher *et al.*, 1989;

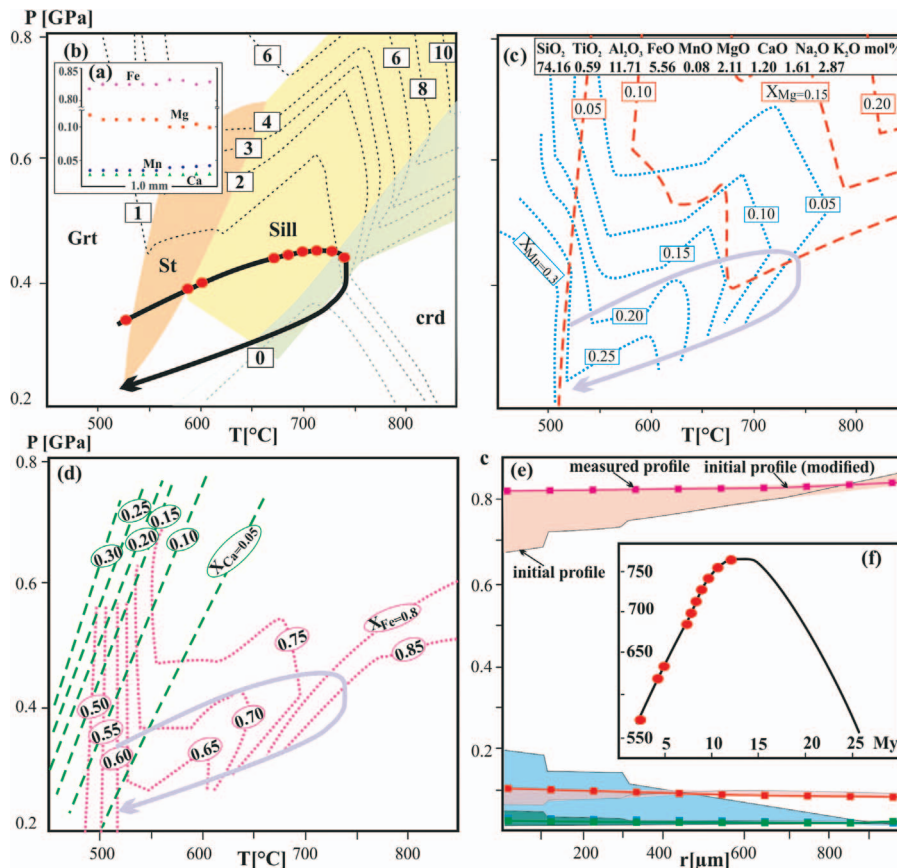


**Fig. 7.** Pressure–temperature path constraint in high-grade amphibolite-granulite facies pelitic rocks from the Damar Belt (Namibia). (a) Measured profile of garnet. (b) Stability fields of the index phase (staurolite, sillimanite, and cordierite) and calculated volume isopleths of garnet. Solid circles along the P–T path indicate the position of garnet growth. (c, d) Compositional isopleths. (e) Best fit between the measured and modified initial profile (vertical axis: c-concentration; horizontal axis: r-normalised radius). (f) T–t path along which diffusion of the initial profiles was quantified.

Thöni & Jagoutz, 1992). The most common minerals in the micaschists are garnet, white mica, biotite, and quartz, though some also contain kyanite, plagioclase, and rarely staurolite. Garnet usually forms porphyroblasts with inclusions of quartz, micas, rutile, ilmenite, plagioclase, staurolite, and kyanite. The porphyroblastic garnets show two distinct growth zones (Fig. 8): a Pre-Alpine central part ( $gt_1$ ) and an Eo-Alpine rim part ( $gt_2$ ) (Schuster *et al.*, 1999; Faryad & Hoinkes, 2003). Both the central and rim parts can be recognised in hand specimens, as their interfaces are followed by inclusions of various phases, especially opaque minerals (ilmenite and graphite).  $Gt_2$  mantles  $gt_1$ , but also forms small idioblastic grains in the matrix. According to Sm/Nd dating the core garnet ( $gt_1$ ) gave a Permian age (269 Ma) and the rim garnet ( $gt_2$ ) was formed during Eo-Alpine (94 Ma) metamorphism (Schuster & Thöni, 1996).

The selected sample (w128) contains large garnet crystals with central garnet ( $gt_1$ ) and rim garnet ( $gt_2$ , Fig. 8). The  $gt_1$  has inclusions of quartz, ilmenite, and muscovite, but the  $gt_2$  may additionally contain plagioclase, paragonite, and rutile. The matrix minerals are composed of quartz, muscovite, paragonite, and biotite. Chlorite is also present in the matrix, but mostly as a replacement product of biotite. The two garnets show prograde zoning with an increase of Mg ( $X_{Mg}$ ) and decrease of Mn towards the rims (Fig. 8a–d). Phase equilibrium calculations, using bulk rock composition, indicated the formation of garnet above 550°C at 0.2 GPa and up to 600°C at 0.65 GPa (P–T path I in Fig. 8e). The P–T path constrained for  $gt_1$  using compositional isopleths indicated crystallisation of its core at 565°C at 0.44 GPa, crossing

the boundary of the garnet–staurolite field and reaching ~600°C at 0.65 GPa, where approximately 6% by volume of garnet forms.

Phase equilibrium calculations to derive P–T path constraints for  $gt_2$  were performed by fractionating  $gt_1$  from the bulk rock composition. In addition to analytical and thermodynamic uncertainties, this approach is subject to inaccuracy due to unclear content of decomposed  $gt_1$ , which could modify the calculated effective bulk composition prior to the formation of  $gt_2$ . The phase diagram section (Fig. 8f) shows garnet formation above 0.6 GPa, where it overlaps the upper boundary of the plagioclase stability field. Based on the intersections of isopleths of measured garnet (Fig. 8d), the garnet starts to form just at the garnet-in boundary (565°C at 0.65 GPa) and its formation continues by isothermal compression or even slight cooling (P–T path II, Fig. 8f) to meet the increase of Ca along the radius up to 0.5 mm. The rest of the garnet, with a radius of up to 1.35 mm, forms by heating with slight decompression.

The isothermal compression at the beginning of the P–T path for the Eo-Alpine ( $gt_2$ ) event can be explained as a result of the partial resorption of  $gr_1$ , which was not included in the effective bulk composition used for the P–T path constraint or by the presence of metastable phases, which controlled the garnet-forming reactions. In the latter case, destabilisation and decomposition of the Ca-bearing phase (plagioclase) had an important role in the formation of grossular-rich garnet. This was due to the pressure increase by the involvement of basement rocks of the Eastern Alps in several subduction-related Eo-Alpine metamorphic events (Miller & Thöni, 1997; Hoinkes *et al.*, 1999; Faryad & Hoinkes, 2003).

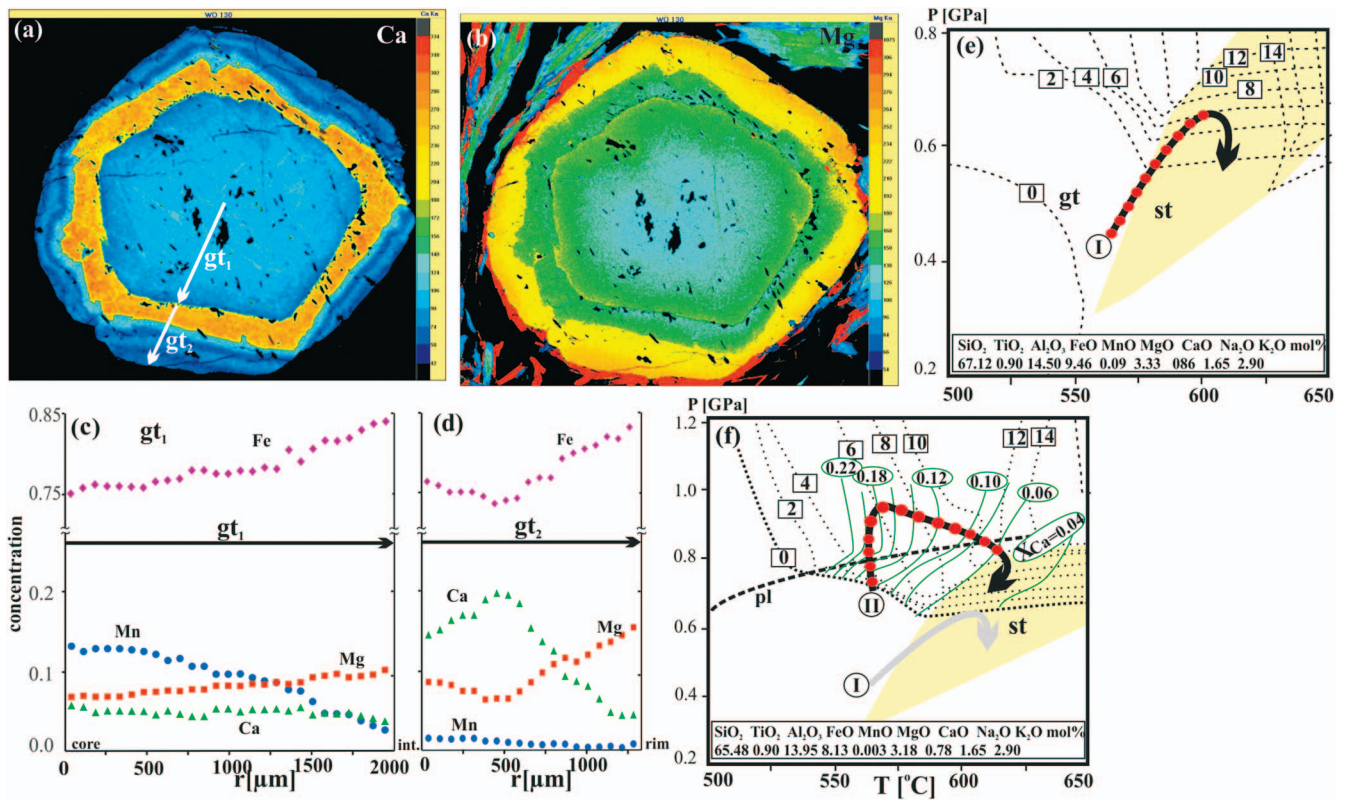


**Fig. 8.** Two (central and rim) garnets from polymetamorphic micaschist in the Eastern Alps. (a–b) X-ray maps of Ca and Mg. Note that Mg shows an increase in both garnets and the interface between the two garnets is followed by inclusion trail. (c–d) Compositional profiles of central and rim garnets in (a). Note the high contrast in composition at the interface (int) between the two garnets. (e) Volume isopleths and P–T path (I) calculated using the bulk rock composition for central garnet (gt<sub>1</sub>). (f) Volume and X<sub>Ca</sub> isopleths and P–T path (II), calculated using the effective bulk rock composition for rim garnet (gt<sub>2</sub>).

## Two garnets formed during a single prograde metamorphic event

Variations in pressure and temperature during metamorphism may lead to periodic change in garnet composition, in that either its growth stops, or it is consumed or replaced by a garnet of different composition. In most cases, the change in the zoning profile is not obvious or may be less visible, but clear examples are known from staurolite zone metapelites when garnet growth stops for some time and is even partially replaced by staurolite (for ref. see Loomis, 1986; Spear, 1993; Pattison & Tinkham, 2009). After the point when the staurolite stability field ends and begins its decomposition, the material released is incorporated into the new growing garnet. Depending on the amount of staurolite replacement, the new garnet rimming the older one may have a sharp boundary with a different composition. As the presence of staurolite in the rock stabilises plagioclase, which takes Ca (Foster, 1986), the composition of the new garnet can be controlled by a complex reaction involving several phases. This means that during formation of the garnet, parts of the reacting phase are decomposed, but others isolate some material, which is difficult to quantify. Details about the interaction of garnet and staurolite during formation are discussed in detail elsewhere (e.g. Spear & Pattison, 2017). This phenomenon may lead to an error in the calculation of effective bulk composition, which is commonly used to predict modal amounts and compositional variation of garnet by application of phase equilibrium modelling.

A similar situation to that described above occurs during atoll garnet formation (Rast, 1965; Smellie, 1974; Homam, 2003; Cheng et al., 2007; Faryad et al., 2010; Ruiz Cruz, 2011). The textural

relations and mechanism of atoll garnet formation have been described for low- to medium-temperature eclogite (Fig. 9), which contains well-preserved growth zoning in full garnet not affected by atollisation (Faryad et al., 2010; Kulhánek et al., 2021). Formation of atoll garnet is explained by fluid infiltration through microfractures in the outer shell of garnet, by which the core of garnet is dissolved, and part of the released material is incorporated into the new garnet overgrowing the inner and outer rim. Depending on the extent of this process, a significant change in composition between the earlier formed central part and outer rim part of garnet grain can occur. Although the dissolved amount of garnet is possible to quantify by image analyses of compositional maps (Kulhánek et al., 2021), the precise time segment for the change in the effective bulk composition during P–T increase needs detailed analyses of the atoll formation and P–T evolution.

Figure 9a–c shows compositional profiles and X-ray maps of a full garnet occurring in an eclogite-facies rock with atoll garnet (Fig. 9d). The rock is formed by garnet (up to 68 vol. %), amphibole (~20 vol. %), and small and accessory amounts of quartz, white mica, talc, rutile/ilmenite, epidote, albite, and chlorite. Compositional maps show a central (gt<sub>1</sub>) and an outer (gt<sub>2</sub>) zone with sharp changes of Ca, Fe, and Mg across their interface. Manganese shows a continuous decrease towards the rims in both zones. The content of Fe shows first an increase with the contact to gt<sub>2</sub>, followed by a decrease towards the rim in gt<sub>2</sub>. Phase equilibrium modelling by Perple\_X with using the bulk rock composition (Kulhánek et al., 2021) and P–T path constraint by CZGM (Fig. 9e) indicate a continuous growth from garnet gt<sub>1</sub> to garnet gt<sub>2</sub> with rapid

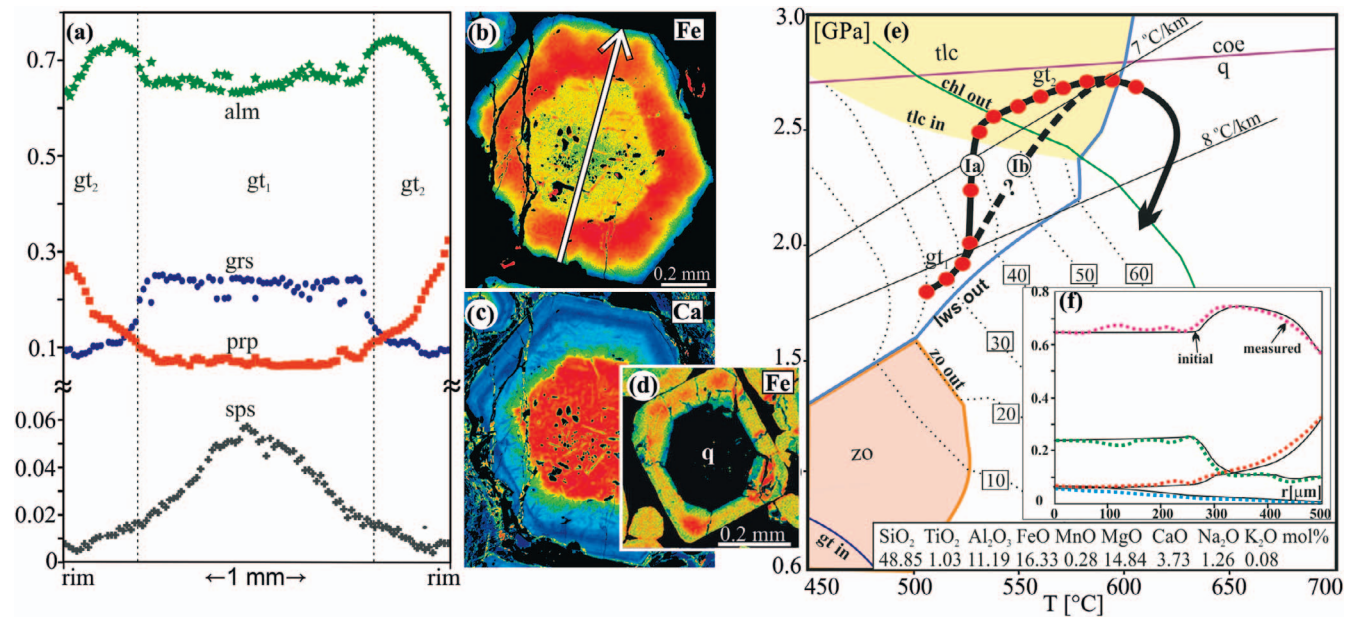


**Fig. 9.** Compositional zoning in garnet and P–T path constraint in eclogite facies metabasite with atoll textures (Kulhánek et al., 2021). (a) Compositional profiles across full (non-atoll) garnet in (b, c). Note that the two central (gt<sub>1</sub>) and rim (gt<sub>2</sub>) zones in garnet (b, c) have contrasting compositions. (d) Compositional map of an atoll garnet, now filled with quartz. (e) Volume isopleths and mineral stability fields of zoisite, lawsonite, talc, chlorite, and garnet. In addition to amphibole, small amounts of mica and rutile/ilmenite are also present. (f) Best fits between measured and calculated (initial) profiles.

compositional changes as seen in Fig. 9a. Pressure–temperature conditions for the outermost rim composition of garnet in these rocks are consistent with those obtained for eclogite with non-atoll garnet and by using exchange thermobarometry with omphacite (Konopásek, 1998; Massonne & Kopp, 2005; Faryad et al., 2010; Collett et al., 2017). As the growing zonation in the measured garnet was not or only insignificantly modified, the sharp but continuous compositional change from gt<sub>1</sub> to gt<sub>2</sub> can be due to the resorption of the garnet core and a change of the effective bulk chemistry. We assume that the sharp change of the P–T path (Ia) with an increase of pressures from ~2.0 to 2.5 GPa at around 525°C, which deviates from the path of continuous burial and heating (dashed line, Ib) to peak pressure and temperature conditions, was due to change of the fractionated bulk composition, which was not considered for the phase diagram calculations.

### Two garnets formed during subduction and subsequent heating during collision

An amphibolite or granulite facies overprint in HP and UHP rocks during their exhumation, known from many orogenic belts (e.g. Central Alps, Wiederkehr et al., 2008; the Western Gneiss Region, Walsh & Hacker, 2004; North Qaidam, Hu et al., 2015; the Bohemian Massif, Faryad & Cuthbert, 2020) could lead to the growth or overgrowth of new garnet of a different composition from that formed under the original HP or UHP conditions. In low-grade rocks, e.g. blueschist facies metapelite with amphibolite facies overprinting, it is easy to recognise the two different garnets and constrain the P–T path for both metamorphic stages (Cruciani et al., 2022). However, amphibolite-granulite facies overprinting results in the modification of the zoning profile, erasing possible composition differences between the two garnets. Possible preservation of zoning in garnet may depend heavily on the temperature reached by the rock and the duration time of the heating process; however, the whole bulk rock chemistry and

thus the proportion of main components in the garnet also play an important role. Figure 10 shows an example of garnets from two samples (RJ34–13 and F103–10) of felsic (quartz-feldspathic) granulite from the Bohemian Massif (Jedlicka et al., 2015). The samples were taken from a single granulite body in the same outcrop, meaning that they share the same metamorphic history. However, sample F103–10 has a better-preserved zoning profile in garnet with higher grossular, but lower almandine content compared to sample RJ34–13. Note that the grain sizes of garnet from both samples are nearly identical. The two samples differ from each other mostly by the whole bulk rock composition, mainly by the molar contents of Fe, Mn, Mg, and Ca; the highest Ca ratio (Fe:Mn:Mg:Ca = 0.4:0.01:0.31:0.28) occurs in sample F103–10 and the lowest (0.47:0.01:0.34:0.18) in sample RJ34–13. Despite similar Mn ratios in the bulk rock of both samples, stronger zoning with high spessartine contents in the core is preserved in garnet from sample F103–10, with a high-Ca-ratio. Another noticeable feature of these garnets is the complex or multiple zoning. Detailed investigation of the trace element distribution has indicated the formation of these garnets in two stages, with the core (grt<sub>1</sub>) having formed during subduction to (U)HP conditions and the rim (grt<sub>2</sub>) during collision under UHT conditions (Jedlicka et al., 2015). These two garnets were recognisable by the presence of central and annular peaks of yttrium + heavy rare earth elements (Y + HREEs, Fig. 10c). The annular peaks, separating grt<sub>1</sub> from grt<sub>2</sub>, can be explained by partial decomposition of (U)HP garnet during exhumation, where yttrium + rare earth elements released into the matrix were incorporated into the new garnet. The preservation of Y + HREE peaks was due to the slow diffusion coefficient of these elements (Carlson et al., 2014) compared to those of the major elements in garnet (Chakraborty & Ganguly, 1992; Schwandt et al., 1996; Vielzeuf et al., 2005; Carlson, 2006). Therefore, any possible compositional gradient of major elements at the interface between the two garnets could be easily modified under the conditions of granulite facies.

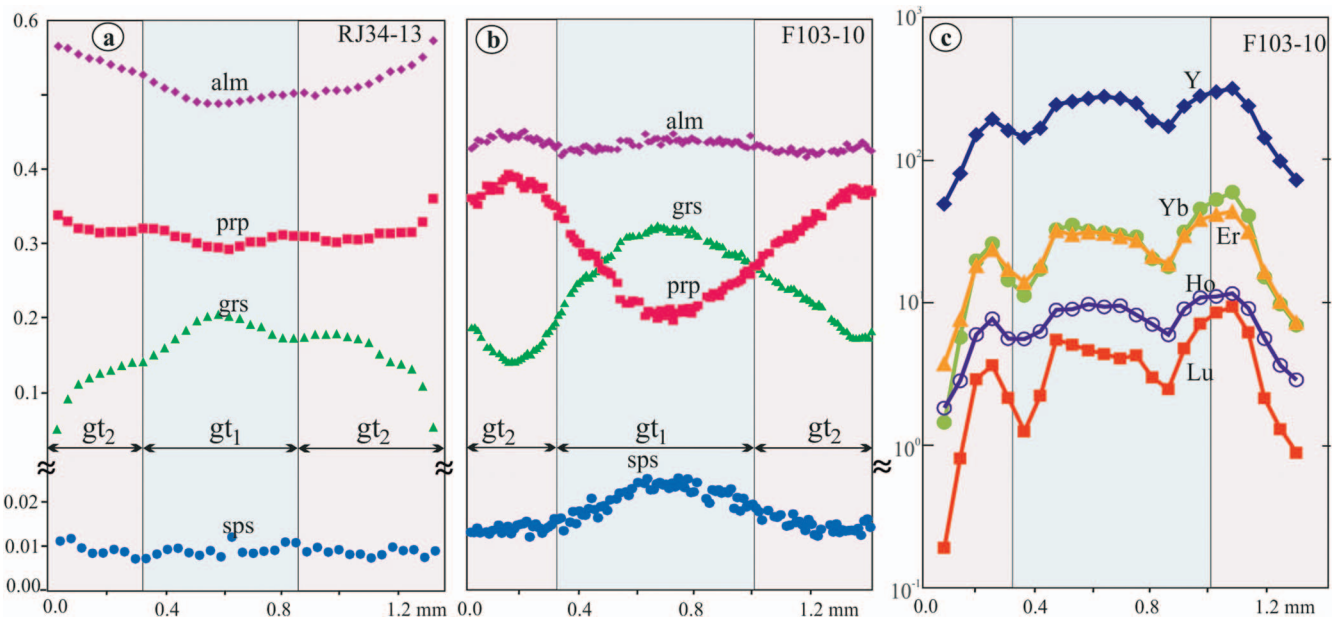


**Fig. 10.** Preservation of growth zoning from two samples (RJ34-13 and F103-10) of felsic granulite from the Bohemian Massif (Jedlicka *et al.*, 2015). (a and b) Major component ratio vs rim-core-rim profile. Both samples come from a single granulite body and from the same outcrop. For the difference in major component ratios in these two samples see text. (c) Concentrations of Y and selected HREE (ppm in logarithmic scale) along the garnet profile in (b) indicate two central annular peaks for gt<sub>1</sub> and gt<sub>2</sub>.

## DELAY IN GARNET CRYSTALLISATION DURING METAMORPHISM

Late formation of garnet in metamorphic rock compared to the predicted one by phase equilibrium modelling is a commonly recognised phenomenon in metamorphic petrology and can be explained as the result of kinetic barriers due to the presence of metastable reactants (Pattison *et al.*, 2011), leading to garnet's episodic growth rather than continuous zoning (Carlson *et al.*, 2015). However, the formation of new minerals in dry rocks is, in addition to the pressure and temperature changes, controlled by deformation and fluid access, which facilitate the breakdown and/or creation of minerals (Ferry, 1979; Austrheim, 1987; Connolly & Thompson, 1989; Faryad *et al.*, 2019, 2022). Accordingly, a lack of fluid will result in the incomplete transformation of minerals and preservation of metastable (relict) phases, which isolate parts of the bulk rock chemistry but would inadvertently be included in phase equilibrium modelling and the prediction of mineral formation. In contrast to pelitic rocks, where growing zonation in garnet follow the bulk rock fractionation, here, zonation in garnet is controlled by the rate of decomposition and release of material from the relict phases. Delayed fluid access to the rock results in a shift in P-T conditions for mineral formation and related garnet-forming reactions, which are different from those during prograde metamorphism (see John & Schenk, 2003; Austrheim, 2013).

Compositional relations of garnet in mafic rock that resisted recrystallisation to coesite eclogite have been described for a rock from Papua New Guinea (Faryad *et al.*, 2019). The rock contains garnet grains with two zones (central: gt<sub>1</sub> and rim: gt<sub>2</sub>) that differ by a sharp change in composition (Fig. 11a and b). The central garnet with a diameter of ~0.6 mm has a flat zoning of major components with a decrease of Mg and increase of Ca towards the rim. The result of phase equilibrium modelling (Fig. 11c) indicates a formation of about 45 vol. % garnet (gt<sub>1</sub>) at a peak pressure/temperature of ~2.8 GPa at 670°C. Based on the calculated compositional isopleths, the garnet should have strong

zoning with a decrease of Ca concentration from 0.4 in the core to 0.1 in the rim (Fig. 11c). The results of diffusion modelling show that the peak temperature or time duration were not enough to homogenise the high compositional gradient along the interface of the two garnets. This suggests that the core of gr<sub>1</sub> did not homogenize either and the formation of the whole garnet (gt<sub>1</sub>) occurred near peak pressure conditions with a Ca concentration of ~0.1 with a further decrease to the outermost rim. Although the garnet has a relatively regular (idioblastic) shape, its rims show various degrees of embayment, suggesting some resorption before growing gt<sub>2</sub>. Based on mineral stability fields (formation of amphibole, paragonite, etc.), this resorption occurred during decompression with minor cooling.

The formation of gt<sub>2</sub> was calculated using the effective bulk composition obtained by removing gt<sub>1</sub> from the whole bulk rock chemistry. The results show formation of this garnet by heating (up to 750°C) that occurred after partial decompression from 2.7 to 1.7 GPa. By combining these results with Lu-Hf dating of garnet (Zirakparvar *et al.*, 2011), the ages of 8.0 and 7.1 Ma for gt<sub>1</sub> and gt<sub>2</sub> formation are considered (Faryad *et al.*, 2019). Diffusion modelling applied to the compositional jump between the two garnets indicates a very short-term (0.3 My) heating to 750°C and cooling during this process. Such a process of heating after partial exhumation of deep subducted rocks is common in many orogens and is typically interpreted as the result of slab breakoff or slab rollback (Sizova *et al.*, 2019; Faryad & Cuthbert, 2020; Chowdhury *et al.*, 2021).

## DISCUSSION AND CONCLUDING REMARKS

The results of this study applied to garnets in natural rocks metamorphosed in different grades and geotectonic settings indicate a number of limitations in terms of constraining P-T trajectories using only phase diagram calculations. Here, we summarise the results and highlight possible solutions for P-T constraint and explain the origin of garnet zoning and its modification during

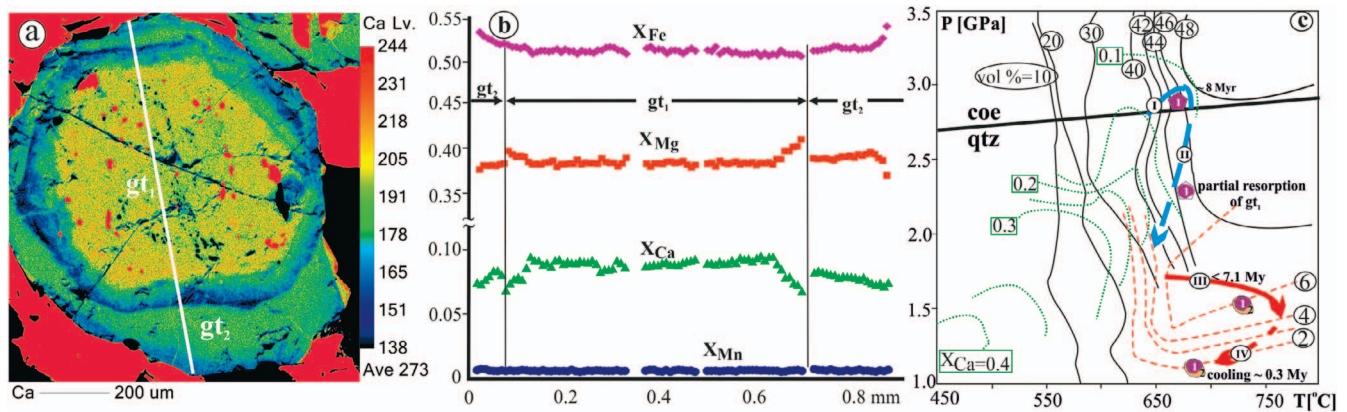


**Fig. 11.** Compositional relations and P–T paths of two garnets in coesite eclogite from Papua New Guinea (Faryad et al., 2019). (a) X-ray map of Ca concentration and compositional profiles (b) of central ( $gt_1$ ) and rim ( $gt_2$ ) garnets. Garnet ( $gt_1$ ) contains inclusions of omphacite, apatite (both in red), and quartz (black). Note the partially resorbed rims of  $gt_1$ . (c) Summary of P–T–t evolution for  $gt_1$  and  $gt_2$  in coesite eclogite. Volume isopleths of  $gt_1$  (solid lines) and  $gt_2$  (dashed lines) were calculated using *Perple\_X*. The isopleths of the Ca ratio show values of  $X_{\text{Ca}} = 0.4$  near the  $gt$ -in field and  $X_{\text{Ca}} = 0.1$  at peak pressures. Isopleths for  $gt_2$  were calculated after fractionation of  $gt_1$ . I–IV are the prograde and retrograde (with resorption) P–T paths of  $gt_1$  and  $gt_2$ , respectively. Age data for  $gt_1$  and  $gt_2$  are from Baldwin et al. (2004) and Zirkparvar et al. (2011). The T–t path for heating and cooling was calculated using CZGM.

metamorphism. We first outline the P–T path constraints in low-grade rocks where prograde zoning in garnet was either not at all or insignificantly affected by diffusion. Then, we discuss the rocks, in which garnet formation did not follow the whole bulk rock fractionation, including the garnet formation during multiple metamorphic events/stage or when garnet crystallised later than the garnet-in boundary. Finally, we outline both the P–T and temperature–time (T–t) path constraints in high-grade rocks with partially or totally homogenised zoning in garnet created during its crystallisation.

## GARNET ZONING IN LOW- TO MEDIUM-GRADE ROCKS

Comparison of a measured profile in garnet with that calculated by phase-equilibrium modelling commonly allows constraint of the P–T path of prograde metamorphism, if the garnet zoning was not modified by diffusion. To test possible modification of the zoning profile in the measured garnet, the best fits between measured and calculated profiles must be obtained using CZGM software to derive the peak temperature estimated by the phase-equilibrium modelling. Moreover, any information about absolute ages or preliminary time duration of metamorphism will additionally improve the quantification of the diffusion of the zoning profile. Additional complexity regarding best fits and P–T constraints can arise if the core composition in the measured garnet is shifted to higher temperatures or pressures from the calculated garnet-in boundary, calculated by phase diagram modelling. The shift between the measured and calculated cores can be a result of either the cut effect, reaction overstepping, or the delay of fluid access to dry rocks during metamorphism. In the case of the cut effect, a portion of the information about the core composition of garnet is missing. A similar situation occurs if the analysed garnet was created later than its nucleation at the calculated garnet-in boundary. In that case, the formation of garnet is assumed to have followed the crystal size distribution, in which the largest grains crystallised first and the smallest later. In the case of reaction overstepping, the mineral formation may not follow the bulk rock fractionation, thus the irregular flux of material may lead to oscillating zonation in garnet or

to the formation of multiple domains in garnet with different concentrations of one or more elements. The best fit solution for the measured and calculated compositional profiles for the last two garnet-forming mechanisms (reaction overstepping and delay of fluid access to dry rocks) is similar to that of the cut effect, as shown in Fig. 3. The P–T path section obtained for the measured profile in such garnet will coincide with part of the whole P–T path calculated using phase diagram and bulk rock composition.

A delay in recrystallisation that often occurs in dry igneous or crystalline rocks is a special case, in which the garnet-forming reactions are controlled by fluid access and material released by partial replacement of original minerals during metamorphism. The fluid access after reaching higher temperatures and/or pressures within garnet stability (i.e. above the garnet-in boundary) will result in the rapid growth of garnet, and the composition of garnet will be controlled by the availability of material released by the decomposition of the original minerals in the rocks. The best example is the flat compositional zoning profiles shown in Fig. 8, which suggest the rapid growth of garnet as a result of deformation and fluid flux into the rock that occurred under coesite-facies conditions. In less-recrystallised rocks (i.e. gabbro and other igneous rocks), a corona garnet forms along the interface of two or more phases, which controls its overall composition (e.g. Proyer & Postl, 2010). Partial decomposition of the original phases that isolate part of the bulk rock composition will result in the formation of garnet with different growth zoning from that calculated using the whole bulk composition.

## GARNET FORMED BY POLYMETAMORPHIC EVENTS OR MULTISTAGE GROWING

Two garnet generations (1, 2) can be well recognised in metamorphic rocks if they were formed under different pressure and temperature conditions that stabilised garnets of different compositions (Fig. 9). In the case of polymetamorphic rocks, the P–T path for the first event (garnet 1) can be calculated using the whole bulk rock composition, similar to that for a single metamorphic event. However, to calculate the P–T path of the second metamorphic event (garnet 2), the effective bulk composition by the reduction of garnet (1) is needed. It should be noted that the

P–T path calculation for the second event is subject to error due to the uncertainty in the calculated effective bulk rock chemistry and possible resorption of garnet (1) or release of elements into the matrix that stabilises the new garnet (2). Yet, if a compositional jump across the interface between the two garnets is developed, this can be easily modified due to the high compositional gradient along the small distance, even in low-grade rocks. In such a case, the diffusion modelling approach can allow the determination of the time constraints (i.e. the duration of the younger garnet-forming process) for modification of this sharp compositional change along the profile (Faryad & Chakraborty, 2005; Faryad, 2012).

In addition to a temporary cessation of garnet growth due to the preferential formation of other phases by metamorphic reactions, e.g. staurolite (Pattison & Tinkham, 2009), the multiple growths of garnet during a single event can occur as a result of the change in the effective bulk rock composition. An example of the latter case would be the presence of two garnet generations or garnets of contrasting compositions, wherein the second garnet formed from partial dissolution of the first garnet due to fluid infiltration along the microfractures and transport of the elements into the matrix (Cheng *et al.*, 2007; Faryad *et al.*, 2010; Kulhánek *et al.*, 2021). In that case, the P–T path, which can be constrained by intersections of isopleths in the phase diagram by using CZGM, will follow the zoning profile in the measured garnet and may result in a sharp change in P or T depending on the transport of major elements from the dissolved core and their reprecipitation along the garnet rim (Fig. 8).

## GARNET ZONING IN HIGH-GRADE METAMORPHIC ROCKS

Garnet in normal pelitic rocks commonly retains the original compositional zoning pattern at temperatures up to 570°C achieved during metamorphism (Fig. 2a and b). In garnet with a higher concentration of Ca, the temperature limit for modification of zoning profile may be shifted up to 600°C (Fig. 9) or even higher. This is due to Ca having the lowest diffusion rate among the major divalent cations in garnet (Chakraborty & Ganguly, 1992; Schwandt *et al.*, 1996; Vielzeuf *et al.*, 2005; Carlson, 2006). A high concentration of Ca in garnet will slow down the overall diffusion within the multicomponent system, even in amphibolite-granulite facies conditions. This was confirmed in felsic granulite (Fig. 10), in which the higher Ca garnet (which is present in the sample with the higher Ca ratio among the major elements: Fe + Mn + Mg + Ca) can be seen to better preserve the prograde zoning.

Possible partial preservation of prograde zoning garnets in high-grade rocks also depends on the relaxation time at peak temperature or further heating after the garnet growth stops. Another parameter controlling intracrystalline diffusion is the distance or size of the garnet. A selection of large grains of garnet with isometric shape is important for the reconstruction of the P–T trajectory in high-grade rocks; however, it is also essential to know when the garnet growth stopped and if the host rock was subject to further heating. Any information about the time of garnet crystallisation (absolute age) or subsequent heating will additionally improve the P–T constraint of the rock. For example, an increase of temperature after the garnet growing stops should lead to homogenisation of the core-to-rim zoning profiles; mainly resulting in the modification of the rim composition of garnet, which tends to be in equilibrium with the surrounding matrix

phases. In the case that heating occurred after partial decompression, in which a garnet of different compositions had stabilised, using such garnet for the P–T estimate will give ‘mixed results’ both in terms of pressure and temperature conditions. This is a common case for garnet formed in high-pressure rocks along a subduction zone with a relatively cool thermal gradient, with subsequent heating after partial exhumation during collision. The best example of this type of (U)HP garnet that has been partially or totally homogenised during granulite facies conditions occurs in the Bohemian Massif. Pressure–temperature conditions calculated for such garnet with other phases in the matrix have yielded mixed results that are commonly interpreted as high-pressure granulite (Rötzler *et al.*, 2004; O’Brien, 2008; Haifler & Kotková, 2016). Detailed study of major and trace element distributions in such garnet (Jedlicka *et al.*, 2015) has shown the presence of garnet with two zones formed under (U)HP and (UHT) conditions, respectively. In that case, because of the granulite-facies temperature and subsequent cooling, the two garnet generation events could hardly be distinguished by major components due to the extensive diffusional re-homogenisation. Only the Y + HREE distributions indicated the presence of the two garnets, separated by an annular peak. The annular peaks can be explained by the partial decomposition of (U)HP garnet during exhumation, during which yttrium + rare earth elements released into the matrix would be incorporated into the new garnet (Jedlicka *et al.*, 2015).

In addition to the cooling history of high-grade rocks, the results of their diffusion modelling can also be used to estimate the rates of burial (subduction) and exhumation. One important factor for this estimate is whether modification of the garnet rim during the retrograde stage occurred or not. This is because modification of the rim composition of garnet during cooling leads to a loss of information about peak P–T conditions reached by the host rock (Loomis, 1977). In that case, the burial and exhumation rate can be calculated along the pressure axis (which reflects the burial depth) from garnet nucleation to the peak pressure/depth, and back again (Faryad & Chakraborty, 2005; Caddick *et al.*, 2010). This requires an assumption of whether the heating and cooling rates were constant along the entire P–T loop, or whether the rock was relaxed over a period of time, e.g. at peak pressure or temperature conditions. It should also be noted that any relaxation of rocks at high temperature will result in an increase of the burial/exhumation and cooling rates for the rest of the sections of the P–T loop. To overcome this problem, a detailed study on the textural relations of the minerals and their formation in the P–T diagram is needed. The results of time-scale calculations in combination with available isotopic ages of minerals formed at one or more points along the P–T loop can help to achieve better constraint of cooling, burial, and exhumation rates.

## FUNDING

This work was supported by the Czech Science Foundation (project no. 18-03160S) and by the Charles University through project Cooperation.

## ACKNOWLEDGEMENTS

Sumit Chakraborty (Bochum) is thanked for valuable suggestions during the preparation of the manuscript. We thank Alexander Proyer and two anonymous reviewers for constructive comments and helpful review and Gieré, Reto, for editorial handling.

## References

- Anczkiewicz, R., Chakraborty, S., Dasgupta, S. & Mukhopadhyay, D. (2014). Duration of prograde metamorphism in the inverted Barrovian sequence, Sikkim Himalaya, India. *Mineralogical Magazine* **77**, 591.
- Austrheim, H. (1987). Eclogitization of lower crustal granulites by fluid migration through shear zones. *Earth and Planetary Science Letters* **81**, 221–232. [https://doi.org/10.1016/0012-821X\(87\)90158-0](https://doi.org/10.1016/0012-821X(87)90158-0).
- Austrheim, H. (2013). Fluid and deformation induced metamorphic processes around Moho beneath continent collision zones: examples from the exposed root zone of the Caledonian mountain belt, W-Norway. *Tectonophysics* **609**, 620–635. <https://doi.org/10.1016/j.tecto.2013.08.030>.
- Baldwin, S. L., Monteleone, B., Webb, L. E., Fitzgerald, P. G., Grove, M. & Hill, E. J. (2004). Pliocene eclogite exhumation at plate tectonic rates in eastern Papua New Guinea. *Nature* **431**, 263–267. <https://doi.org/10.1038/nature02846>.
- Baldwin, J. A., Powell, R., Brown, M., Moraes, R. & Fuck, R. A. (2005). Modelling of mineral equilibria in ultrahigh-temperature metamorphic rocks from the Anápolis-Itaúcu Complex, central Brazil. *Journal of Metamorphic Geology* **23**, 511–531. <https://doi.org/10.1111/j.1525-1314.2005.00591.x>.
- Benisek, A., Dachs, E. & Kroll, H. (2010). A ternary feldspar-mixing model based on calorimetric data: development and application. *Contributions to Mineralogy and Petrology* **160**, 327–337. <https://doi.org/10.1007/s00410-009-0480-8>.
- Caddick, M., Konopasek, J. & Thompson, A. B. (2010). Preservation of garnet growth zoning and the duration of prograde metamorphism. *Journal of Petrology* **51**, 2327–2347. <https://doi.org/10.1093/petrology/egq059>.
- de Capitani, C. (1994). Gleichgewichts-Phasendiagramme: theorie und software. *Beihefte zum European Journal of Mineralogy* **72**, *Jahrestagung der Deutschen Mineralogischen Gesellschaft*, 6, 48.
- de Capitani, C. & Brown, T. H. (1987). The computation of chemical equilibrium in complex systems containing non-ideal solutions. *Geochimica et Cosmochimica Acta* **51**, 2639–2652. [https://doi.org/10.1016/0016-7037\(87\)90145-1](https://doi.org/10.1016/0016-7037(87)90145-1).
- de Capitani, C. & Petrakakis, K. (2010). The computation of equilibrium assemblage diagrams with Theriak-/Domino software. *American Mineralogist* **95**, 1006–1016. <https://doi.org/10.2138/am.2010.3354>.
- Carlson, W. D. (2006). Rates of Fe, Mg, Mn, and Ca diffusion in garnet. *American Mineralogist* **91**, 1–11. <https://doi.org/10.2138/am.2006.2043>.
- Carlson, W. D., Pattison, D. R. M. & Caddick, M. J. (2015). Beyond the equilibrium paradigm: how consideration of kinetics enhances metamorphic interpretation. *American Mineralogist* **100**, 1659–1667. <https://doi.org/10.2138/am-2015-5097>.
- Carlson, W. D., Gale, J. D. & Wright, K. (2014). Incorporation of Y and REEs in aluminosilicate garnet: energetics from atomistic simulation. *American Mineralogist* **99**, 1022–1034. <https://doi.org/10.2138/am.2014.4720>.
- Castro, A. E. & Spear, F. S. (2017). Reaction overstepping and re-evaluation of peak P-T conditions of the blueschist unit Sifnos, Greece: implications for the Cyclades subduction zone. *International Geology Review* **59**, 548–562. <https://doi.org/10.1080/00206814.2016.1200499>.
- Chakraborty, S. & Ganguly, J. (1991). Compositional zoning and cation diffusion in garnet. In: Ganguly, J. (ed.) *Diffusion, Atomic Ordering and Mass Transport: Selected Topics in Geochemistry. Advances in Physical Geochemistry* **8**, 120–175. [https://doi.org/10.1007/978-1-4613-9019-0\\_4](https://doi.org/10.1007/978-1-4613-9019-0_4).
- Chakraborty, S. & Ganguly, J. (1992). Cation diffusion in aluminosilicate garnets: experimental determination in spessartine-almandine diffusion couples, evaluation of effective binary, diffusion coefficients, and applications. *Contributions to Mineralogy and Petrology* **111**, 74–86. <https://doi.org/10.1007/BF00296579>.
- Chakraborty, S., Anczkiewicz, R., Gaidies, F., Rubatto, D., Sorcar, N., Faak, K., Mukhopadhyay, D. K. & Dasgupta, S. (2016). A review of thermal history and timescales of tectonometamorphic processes in Sikkim Himalaya (NE India) and implications for rates of metamorphic processes. *Journal of Metamorphic Geology* **34**, 785–803. <https://doi.org/10.1111/jmg.12200>.
- Cheng, H., Nakamura, E., Kobayashi, K. & Zhou, Z. (2007). Origin of atoll garnets in eclogites and implications for the redistribution of trace elements during slab exhumation in a continental subduction zone. *American Mineralogist* **92**, 1119–1129. <https://doi.org/10.2138/am.2007.2343>.
- Chowdhury, P., Chakraborty, S. & Gerya, T. V. (2021). Time will tell: secular change in metamorphic timescales and the tectonic implications. *Gondwana Research* **93**, 291–310. <https://doi.org/10.1016/j.gr.2021.02.003>.
- Coggon, R. & Holland, T. J. B. (2002). Mixing properties of phengitic micas and revised garnet–phengite thermobarometers. *Journal of Metamorphic Geology* **20**(7), 683–696. <https://doi.org/10.1046/j.1525-1314.2002.00395.x>.
- Collett, S., Štípská, P., Kusbach, V., Schulmann, K. & Marciniak, G. (2017). Dynamics of Saxothuringian subduction channel/wedge constrained by phase-equilibria modelling and microfabric analysis. *Journal of Metamorphic Geology* **35**, 253–280. <https://doi.org/10.1111/jmg.12226>.
- Connolly, J. A. D. (2005). Computation of phase equilibria by linear programming: a tool for geodynamic modeling and its application to subduction zone decarbonation. *Earth and Planetary Science Letters* **236**, 524–541. <https://doi.org/10.1016/j.epsl.2005.04.033>.
- Connolly, J. A. D. (2009). The geodynamic equation of state: what and how. *Geochemistry, Geophysics, Geosystems* **10**, Q10014. <https://doi.org/10.1029/2009GC002540>.
- Connolly, J. A. D. & Thompson, A. B. (1989). Fluid and enthalpy production during regional metamorphism. *Contributions to Mineralogy and Petrology* **102**, 347–366. <https://doi.org/10.1007/BF00373728>.
- Cruciani, G., Franceschelli, M., Carosi, R. & Montomoli, C. (2022). P-T path from garnet zoning in pelitic schist from NE Sardinia, Italy: further constraints on the metamorphic and tectonic evolution of the north Sardinia Variscan belt. *Lithos* **428–429**, 106836. <https://doi.org/10.1016/j.lithos.2022.106836>.
- Daniel, C. G. & Spear, F. S. (1998). Three-dimensional patterns of garnet nucleation and growth. *Geology* **26**, 505–506. <https://doi.org/10.1130/0091-7613>.
- Dasgupta, S., Ganguly, J. & Neogi, S. (2004). Inverted metamorphic sequence in the Sikkim Himalayas: crystallisation history, P-T gradient and implications. *Journal of Metamorphic Geology* **22**, 395–412. <https://doi.org/10.1111/j.1525-1314.2004.00522.x>.
- Dempster, T. J., Gilmour, M. I. & Chung, P. (2019). The partial equilibration of garnet porphyroblasts in pelitic schists and its control on prograde metamorphism, Glen Roy, Scotland. *Journal of Metamorphic Geology* **37**, 383–399. <https://doi.org/10.1111/jmg.12467>.
- Faryad, S. W. (2012). High-pressure polymetamorphic garnet growth in eclogites from the Mariánské Lázně Complex (Bohemian Massif). *European Journal of Mineralogy* **24**, 483–497. <https://doi.org/10.1127/0935-1221/2012/0024-2184>.

- Faryad, S. W. & Chakraborty, S. (2005). Duration of Eo-Alpine metamorphic events obtained from multicomponent diffusion modeling of garnet: a case study from the Eastern Alps. *Contributions to Mineralogy and Petrology* **150**, 306–318. <https://doi.org/10.1007/s00410-005-0020-0>.
- Faryad, S. W. & Cuthbert, S. J. (2020). High-temperature overprint in (U)HPM rocks exhumed from subduction zones: a product of isothermal decompression or a consequence of slab break-off (slab rollback)? *Earth-Science Reviews* **202**, 103108. <https://doi.org/10.1016/j.earscirev.2020.103108>.
- Faryad, S. W. & Hoinkes, G. (2003). P-T gradient of Eo-Alpine metamorphism within the Austroalpine basement units east of the Tauern Window (Austria). *Mineralogy and Petrology* **77**, 129–159. <https://doi.org/10.1007/s00710-002-0196-1>.
- Faryad, S. W. & Ježek, J. (2019). Compositional zoning in garnet and its modification by diffusion during pressure and temperature changes in metamorphic rocks. *Lithos* **332–333**, 287–295. <https://doi.org/10.1016/j.lithos.2019.03.002>.
- Faryad, S. W., Klápová, H. & Nosál, L. (2010). Mechanism of formation of atoll garnet during high-pressure metamorphism. *Mineralogical Magazine* **74**, 111–126. <https://doi.org/10.1180/minmag.2010.074.1.111>.
- Faryad, S. W., Baldwin, S. L., Jedlička, R. & Ježek, J. (2019). Two-stage garnet growth in coesite eclogite from the southeastern Papua New Guinea (U)HP terrane and its geodynamic significance. *Contributions to Mineralogy and Petrology* **174**, 1–16. <https://doi.org/10.1007/s00410-019-1612-4>.
- Faryad, S. W., Ježek, J. & Kulhánek, J. (2022). P-T path constraint of (U)HP rocks with reaction overstepping during subduction: example from the Western Gneiss Region (Norway). *Journal of Metamorphic Geology* **40**, 1427–1446. <https://doi.org/10.1111/jmg.12680>.
- Ferry, J. M. (1979). Reaction mechanisms, physical conditions, and mass transfer during hydrothermal alteration of mica and feldspar in granitic rocks from south-central Maine, USA. *Contributions to Mineralogy and Petrology* **68**, 125–139. <https://doi.org/10.1007/BF00371895>.
- Florence, F. P. & Spear, F. S. (1991). Effects of diffusional modification of garnet growth zoning on P-T path calculations. *Contributions to Mineralogy and Petrology* **107**, 487–500. <https://doi.org/10.1007/Bf00310683>.
- Foster, C. T. (1986). Thermodynamic models of reactions involving garnet in a sillimanite/staurolite schist. *Mineralogical Magazine* **50**, 427–439. <https://doi.org/10.1180/minmag.1986.050.357.07>.
- Frank, W. (1987) Evolution of the Austroalpine elements in the Cretaceous. In: Flügel H. W. & Faupl P. (eds) *Geodynamics of the Eastern Alps*. Vienna: Franz Deuticke, pp.379–406.
- Gaidies, F. & George, F. (2021). The interfacial energy penalty to crystal growth close to equilibrium. *Geology* **49**(8), 988–992. <https://doi.org/10.1130/G48715.1>.
- Gaidies, F., Abart, R., de Capitani, C., Schuster, R., Connolly, J. A. D. & Reusser, E. (2006). Characterization of polymetamorphism in the Austroalpine basement east of the Tauern window using garnet isopleth thermobarometry. *Journal of Metamorphic Geology* **24**, 451–475. <https://doi.org/10.1111/j.1525-1314.2006.00648.x>.
- Gaidies, F., de Capitani, C. & Abart, R. (2008). THERIA\_G: a software program to numerically model prograde garnet growth. *Contributions to Mineralogy and Petrology* **155**, 657–671. <https://doi.org/10.1007/s00410-007-0263-z>.
- Gaidies, F., Petley-Ragan, A., Chakraborty, S., Dasgupta, S. & Jones, P. (2015). Constraining the conditions of Barrovian metamorphism in Sikkim, India: P–T paths of garnet crystallisation in the Lesser Himalayan Belt. *Journal of Metamorphic Geology* **33**, 23–44. <https://doi.org/10.1111/jmg.12108>.
- Ganguly, J., Cheng, W. & Chakraborty, S. (1998). Cation diffusion in aluminosilicate garnets: experimental determination in pyrope-almandine diffusion couples. *Contributions to Mineralogy and Petrology* **131**, 171–180. <https://doi.org/10.1007/s004100050386>.
- Haifler, J. & Kotková, J. (2016). UHP-UHT peak conditions and near-adiabatic exhumation path of diamond-bearing garnet-clinopyroxene rocks from the Eger Crystalline Complex, North Bohemian Massif. *Lithos* **248–251**, 366–381. <https://doi.org/10.1016/j.lithos.2016.02.001>.
- Hoinkes, G., Koller, F., Rantitsch, G., Dachs, E., Höck, V., Neubauer, F. & Schuster, R. (1999). Alpine metamorphism of the Eastern Alps. *Schweizerische Mineralogische und Petrographische Mitteilungen* **79**, 155–181.
- Holland, T. J. B. & Powell, R. (1998). An internally consistent thermodynamic data set for phases of petrological interest. *Journal of Metamorphic Geology* **16**, 309–343. <https://doi.org/10.1111/j.1525-1314.1998.00140.x>.
- Holland, T. & Powell, R. (2003). Activity-compositions relations for phases in petrological calculations: An asymmetric multicomponent formulation. *Contributions to Mineralogy and Petrology* **145**, 492–501.
- Holland, T. J. B. & Powell, R. (2011). An improved and extended internally consistent thermodynamic dataset for phases of petrological interest, involving a new equation of state for solids. *Journal of Metamorphic Geology* **29**, 333–383. <https://doi.org/10.1111/j.1525-1314.2010.00923.x>.
- Homam, S. M. (2003). Formation of atoll garnet in the Ardara aureole, NW Ireland. *Journal of Sciences, Islamic Republic of Iran* **14**, 247–258.
- Hu, R., Wijbrans, J., Brouwer, F., Zhao, L., Wang, M. & Qiu, H. (2015). Retrograde metamorphism of the eclogite in North Qaidam, western China: constraints by joint  $^{40}\text{Ar}/^{39}\text{Ar}$  in vacuo crushing and stepped heating. *Geoscience Frontiers* **6**, 759–770. <https://doi.org/10.1016/j.gsf.2014.09.005>.
- Jedlička, R., Faryad, S. W. & Hauzenberger, C. (2015). Prograde metamorphic history of UHP granulites from the Moldanubian Zone (Bohemian Massif) revealed by major element and Y + REE zoning in garnets. *Journal of Petrology* **56**, 2069–2088. <https://doi.org/10.1093/petrology/egv066>.
- John, T. & Schenk, V. (2003). Partial eclogitisation of gabbroic rocks in a late Precambrian subduction zone (Zambia): prograde metamorphism triggered by fluid infiltration. *Contributions to Mineralogy and Petrology* **146**, 174–191. <https://doi.org/10.1007/s00410-003-0492-8>.
- Jung, S., Brandt, S., Bast, R., Scerer, E. E. & Brend, J. (2019). Metamorphic petrology of a high-T/low-P granulite terrane (Damara belt, Namibia)—constraints from pseudosection modelling and high-precision Lu–Hf garnet-whole rock dating. *Journal of Metamorphic Geology* **37**, 41–69. <https://doi.org/10.1111/jmg.12448>.
- Konopásek, J. (1998). Formation and destabilization of the high pressure assemblage garnet-phengite-paragonite (Krušné hory Mountains, Bohemian Massif): the significance of the Tschermak substitution in the metamorphism of pelitic rocks. *Lithos* **42**, 269–284. [https://doi.org/10.1016/S0024-4937\(97\)00046-7](https://doi.org/10.1016/S0024-4937(97)00046-7).
- Kulhánek, J., Faryad, S. W., Jedlička, R. & Svojtka, M. (2021). Dissolution and reprecipitation of garnet during eclogite facies metamorphism: major and trace elements budget during atoll garnet formation. *Journal of Petrology* **62**(11), 1–22. <https://doi.org/10.1093/petrology/egab077>.
- Lasaga, A. C. (1979). The treatment of multi-component diffusion and ion pairs in diagenetic fluxes. *American Journal of Science* **279**, 324–346.

- Lasaga, A. (1998). *Kinetic Theory in the Earth Sciences*. Princeton University Press. 728 pp., <https://doi.org/10.1515/9781400864874>.
- Loomis, T. P. (1977). Kinetics of a garnet granulite reaction. *Contributions to Mineralogy and Petrology* **62**, 1–22. <https://doi.org/10.1007/BF00371024>.
- Loomis, T. P. (1979). A natural example of metastable reactions involving garnet and sillimanite. *Journal of Petrology* **20**, 1979, 271–292. <https://doi.org/10.1093/petrology/20.2.271>.
- Loomis, T. P. (1986). Metamorphism of metapelites: calculations of equilibrium assemblages and numerical simulations of the crystallisation of garnet. *Journal of Metamorphic Geology* **4**, 201–229. <https://doi.org/10.1111/j.1525-1314.1986.tb00347.x>.
- Loomis, T. P., Ganguly, J. & Elphick, S. C. (1985). Experimental determination of cation diffusivities in aluminosilicate garnets II. Multicomponent simulation and tracer diffusion coefficients. *Contribution to Mineralogy and Petrology* **90**, 45–51. <https://doi.org/10.1007/BF00373040>.
- Mahar, E. M., Baker, J. M., Powell, R., Holland, T. J. B. & Howell, N. (1997). The effect of Mn on mineral stability in metapelites. *Journal of Metamorphic Geology* **15**, 223–238. <https://doi.org/10.1111/j.1525-1314.1997.00011.x>.
- Massonne, H.-J. & Kopp, J. (2005). A low-variance mineral assemblage with talc and phengite in an eclogite from the Saxonian Erzgebirge, Central Europe, and its P–T evolution. *Journal of Petrology* **46**, 355–375. <https://doi.org/10.1093/petrology/egh079>.
- Miller, C. & Thöni, M. (1997). Eo-Alpine eclogitisation of Permian MORB-type gabbros in the Koralpe (Eastern Alps, Austria): new geochronological, geochemical and petrological data. *Chemical Geology* **137**, 283–310. [https://doi.org/10.1016/S0009-2541\(96\)00165-9](https://doi.org/10.1016/S0009-2541(96)00165-9).
- O'Brien, P. J. (2008). Challenges in high-pressure granulite metamorphism: reaction textures, compositional zoning, ages and tectonic interpretation with examples from the Bohemian Massif. *Journal of Metamorphic Geology* **26**, 235–251. <https://doi.org/10.1111/j.1525-1314.2007.00758.x>.
- Onsager, L. (1945). Theories and problems of liquid diffusion. *Annals of the New York Academy of Sciences* **46**, 241–265. <https://doi.org/10.1111/j.1749-6632.1945.tb36170.x>.
- Pattison, D. R. M. & Tinkham, D. T. (2009). Interplay between equilibrium and kinetics in prograde metamorphism of pelites: an example from the Nelson aureole, British Columbia. *Journal of Metamorphic Geology* **27**, 249–279. <https://doi.org/10.1111/j.1525-1314.2009.00816.x>.
- Pattison, D. R. M., de Capitani, C. & Gaidies, F. (2011). Petrologic consequences of variations in metamorphic reaction affinity. *Journal of Metamorphic Geology* **29**, 953–977. <https://doi.org/10.1111/j.1525-1314.2011.00950.x>.
- Perchuk, A. L. & Gerya, T. V. (2005). Subsidence and exhumation dynamics of eclogites in the Yukon–Tanana terrane, Canadian cordillera: Petrological reconstructions and geodynamic modeling. *Petrology* **13**(3), 280–294.
- Proyer, A. & Postl, W. (2010). Eclogitized gabbros from Gressenberg, Koralpe, Austria: transformation phenomena and their interpretation. *Mitteilungen des naturwissenschaftlichen Vereines für Steiermark* **140**, 45–67.
- Putnis, A., Moore, J., Prent, A. M., Beinlich, A. & Austrheim, H. (2021). Preservation of granulite in a partially eclogitized terrane: metastable phenomena or local pressure variations? *Lithos* **400–401**, 106413.
- Rast, N. (1965) Nucleation and growth of metamorphic minerals. In: Pitcher W. S. & Flinn G. W. (eds) *Controls of Metamorphism*. Edinburgh: Oliver and Boyd, pp.73–102.
- Ratschbacher, L., Frisch, W., Neubauer, F., Schmid, S. M. & Neugebauer, J. (1989). Extension in a compressional orogen: the eastern Alps. *Geology* **17**, 404–407. [https://doi.org/10.1130/0091-7613\(1989\)017<0404:EICOBT>2.3.CO;2](https://doi.org/10.1130/0091-7613(1989)017<0404:EICOBT>2.3.CO;2).
- Rötzler, J., Romer, R. L., Budzinski, H. & Oberhänsli, R. (2004). Ultrahigh-temperature high-pressure granulites from Tirschheim, Saxon Granulite Massif, Germany. *European Journal of Mineralogy* **16**, 917–937. <https://doi.org/10.1127/0935-1221/2004/0016-0917>.
- Ruiz Cruz, M. D. (2011). Origin of atoll garnet in schists from the Alpujrride Complex (central zone of the Betic Cordillera, Spain): implications on the P–T evolution. *Mineralogy and Petrology* **101**(3–4), 245–261. <https://doi.org/10.1007/s00710-011-0147-9>.
- Schuster, R. & Thöni, M. (1996). Permian garnet: indications for a regional Permian metamorphism in the southern part of the Austroalpine basement units. *Mitteilungen der Österreichischen Mineralogischen Gesellschaft* **141**, 219–221.
- Schuster, R., Bernhard, F., Hoinkes, G., Kaindl, R., Koller, F., Leber, T., Melcher, F. & Puhl, J. (1999). Excursion to the Eastern Alps: metamorphism at the eastern end of the Alps–Alpine, Permo-Triassic, Variscan? *Beihefte zum European Journal of Mineralogy* **11**, 111–136.
- Schwandt, C. S., Papike, J. J. & Shearer, C. K. (1996). Trace element zoning in pelitic garnet of the Black Hills, South Dakota. *American Mineralogist* **81**, 1195–1207. <https://doi.org/10.2138/am-1996-9-1018>.
- Sizova, E., Hauzenberger, C., Fritz, H., Faryad, S. W. & Gerya, T. (2019). Late orogenic heating of (ultra) high pressure rocks: slab rollback vs. slab breakoff. *Geosciences* **9**, 499. <https://doi.org/10.3390/geosciences9120499>.
- Smellie, J. A. T. (1974). Formation of atoll garnets from the aureole of the Ardara pluton, Co. Donegal, Ireland. *Mineralogical Magazine* **39**, 878–888. <https://doi.org/10.1180/minmag.1974.039.308.07>.
- Spear, F. S. (1993) *Metamorphic Phase Equilibria and Pressure-Temperature-Time Paths*. Washington, DC: Mineralogical Society of America Monograph, p.799.
- Spear, F. S. & Pattison, D. R. M. (2017). The implications of overstepping for metamorphic assemblage diagrams (MADs). *Chemical Geology* **457**, 38–46. <https://doi.org/10.1016/j.chemgeo.2017.03.011>.
- Spear, F. S. & Wolfe, O. M. (2019). Implications of overstepping of garnet nucleation for geothermometry, geobarometry and P–T path calculations. *Chemical Geology* **530**, 119323. <https://doi.org/10.1016/j.chemgeo.2019.119323>.
- Spear, F. S., Peacock, S. M., Kohn, M. J., Florence, F. P. & Menard, T. (1991). Computer programs for petrologic PT-t path calculations. *American Mineralogist* **76**, 2009–2012.
- Thöni, M. & Jagoutz, E. (1992). Some new aspects of dating eclogite in orogenic belts: Sm–Nd, Rb–Sr and Pb–Pb isotopic results from the Austroalpine Saualpe and Koralpe type-locality (Carinthia/Styria, Southeast Austria). *Geochimica et Cosmochimica Acta* **56**, 347–368. [https://doi.org/10.1016/0016-7037\(92\)90138-9](https://doi.org/10.1016/0016-7037(92)90138-9).
- Vielzeuf, D., Veschambre, M. & Brunet, F. (2005). Oxygen isotope heterogeneities and diffusion profile in composite metamorphic-magmatic garnets from the Pyrenees. *American Mineralogist* **90**, 463–472. <https://doi.org/10.2138/am.2005.1576>.
- Walsh, E. O. & Hacker, B. R. (2004). The fate of subducted continental margins: two-stage exhumation of the high-pressure to ultrahigh-pressure Western Gneiss Region, Norway. *Journal of Metamorphic Geology* **22**, 671–687. <https://doi.org/10.1111/j.1525-1314.2004.00541.x>.

- Waters, D. J. & Lovegrove, D. P. (2002). Assessing the extent of disequilibrium and overstepping of prograde metamorphic reactions in metapelites from the Bushveld Complex aureole, South Africa. *Journal of Metamorphic Geology* **20**(1), 135–149. <https://doi.org/10.1046/j.0263-4929.2001.00350.x>.
- Weller, O. M., St-Onge, M. R., Waters, D. J., Rayner, N., Searle, M. P., Chung, S.-L., Palin, R. M., Lee, Y.-H. & Xu, X. (2013). Quantifying Barrovian metamorphism in the Danba Structural Culmination of eastern Tibet. *Journal of Metamorphic Geology* **31**(9), 909–935. <https://doi.org/10.1111/jmg.12050>.
- White, R. W., Powell, R., Holland, H. D. & Worley, B. (2000). The effect of TiO<sub>2</sub> and Fe<sub>2</sub>O<sub>3</sub> on metapelitic assemblages at greenschist and amphibolite facies conditions: mineral equilibria calculations in the system K<sub>2</sub>O-FeO-MgO-Al<sub>2</sub>O<sub>3</sub>-SiO<sub>2</sub>-H<sub>2</sub>O-TiO<sub>2</sub>-Fe<sub>2</sub>O<sub>3</sub>. *Journal of Metamorphic Geology* **18**, 497–511. <https://doi.org/10.1046/j.1525-1314.2000.00269.x>.
- White, R. W., Pomroy, N. E. & Powell, R. (2005). An in situ metatexite–diatexite transition in upper amphibolite facies rocks from Broken Hill, Australia. *Journal of Metamorphic Geology* **23**, 579–602. <https://doi.org/10.1111/j.1525-1314.2005.00597.x>.
- White, R. W., Powell, R. & Holland, T. J. B. (2007). Progress relating to calculation of partial melting equilibria for metapelites. *Journal of Metamorphic Geology* **25**, 511–527. <https://doi.org/10.1111/j.1525-1314.2007.00711.x>.
- White, R. W., Powell, R., Holland, T. J. B., Johnson, T. E. & Green, E. C. R. (2014). New mineral activity-composition relations for thermodynamic calculations in metapelitic systems. *Journal of Metamorphic Geology* **32**, 261–286. <https://doi.org/10.1111/jmg.12071>.
- Wiederkehr, M., Bousquet, R., Schmid, S. M. & Berger, A. (2008). From subduction to collision: thermal overprint of HP/LT meta-sediments in the north-eastern Lepontine Dome (Swiss Alps) and consequences regarding the tectono-metamorphic evolution of the Alpine orogenic wedge. *Swiss Journal of Geosciences* **101**, 127–155. <https://doi.org/10.1007/s00015-008-1289-6>.
- Zeh, A. & Holness, M. B. (2003). The effect of reaction overstep on garnet microtextures in metapelitic rocks of the Ilesha Schist Belt, SW Nigeria. *Journal of Petrology* **44**, 967–994. <https://doi.org/10.1093/petrology/44.6.967>.
- Zirakparvar, N. A., Baldwin, S. L. & Vervoort, J. D. (2011). Lu-Hf garnet geochronology applied to plate boundary zones: insights from the (U)HP terrane exhumed within the Woodlark Rift. *Earth and Planetary Science Letters* **309**, 56–66. <https://doi.org/10.1016/j.epsl.2011.06.016>.